

Fall 2023

Organic Carbon Decay Mediated by Mesopelagic Microbial Communities

Noah Jonathan Craft
Old Dominion University

Follow this and additional works at: https://digitalcommons.odu.edu/oeas_etds



Part of the [Ecology and Evolutionary Biology Commons](#), [Microbiology Commons](#), and the [Oceanography Commons](#)

Recommended Citation

Craft, Noah J.. "Organic Carbon Decay Mediated by Mesopelagic Microbial Communities" (2023). Master of Science (MS), Thesis, Ocean & Earth Sciences, Old Dominion University, DOI: 10.25777/8f8t-kg44 https://digitalcommons.odu.edu/oeas_etds/195

This Thesis is brought to you for free and open access by the Ocean & Earth Sciences at ODU Digital Commons. It has been accepted for inclusion in OES Theses and Dissertations by an authorized administrator of ODU Digital Commons. For more information, please contact digitalcommons@odu.edu.

**ORGANIC CARBON DECAY MEDIATED BY MESOPELAGIC MICROBIAL
COMMUNITIES**

by

Noah Jonathan Craft
B.S. May 2020, Virginia Wesleyan University

A Thesis Submitted to the Faculty of
Old Dominion University in Partial Fulfillment of the
Requirement for the Degree of

MASTER OF SCIENCE

OCEAN AND EARTH SCIENCES

OLD DOMINION UNIVERSITY
December 2023

Approved by:

Alexander B. Bochdansky (Director)

P. Dreux Chappell (Member)

H. Rodger Harvey (Member)

ABSTRACT

ORGANIC CARBON DECAY MEDIATED BY MESOPELAGIC MICROBIAL COMMUNITIES

Noah Jonathan Craft
Old Dominion University, 2023
Director: Dr. Alexander B. Bochdansky

Substantial remineralization of organic carbon occurs in the mesopelagic zone (i.e., the biological pump), the efficiency of which is responsible for the oceans' capacity to store carbon originally derived from the atmosphere. To better understand how a substrate's composition influences its degradation by mesopelagic microbial communities, we added treatments made of live algal cells, dead particulate organic carbon and dissolved organic carbon from ^{14}C -labeled algal cultures to mesopelagic water collected in-situ. Each incubation took place in the laboratory over a period of months, during which PO^{14}C , DO^{14}C , ATP, prokaryote abundances and biochemical fractions were measured. Three algal species were used: *Emiliana huxleyi*, *Thalassiosira weissflogii* and *Tetraselmis* sp. Prokaryote biomass measured via cell counts and adenosine triphosphate responded quickly to the addition of organic material; peaks in both occurred within four to 10 days in most incubations. Thereafter, prokaryote abundances declined because of organic resource depletion and protist grazing. There were significant differences in decay rates between the live, POC, and DOC fractions, in POC between each species of algae, and in DOC between some algal species. DOC treatments exhibited the most rapid decay, followed by POC and lastly live treatments. *E. huxleyi* POC was initially degraded slower than any other dead substrate (POC or DOC). Our data suggest that carbon decay generally occurs in two significantly different phases: a rapid decay over the first three weeks (or less), followed by a slower, more gradual decline. On a more time-resolved level, the decay rate constants for the

dead treatments rapidly increased and peaked after one to two days. Our results show that the use of a frequently applied, simple exponential function (i.e., first-order kinetics) hardly ever applies and is thus unsuitable for describing the trajectory of organic carbon decay. Lipids decayed more rapidly than proteins, polysaccharides-nucleic acids and the low molecular weight fractions during the first phase of decay. During the second phase, the lipid decay rates were similar to those of the other fractions. Overall, the carbon fraction (POC or DOC) and its status (live or dead) exerted more control over carbon decay rates than the type of algal species.

Copyright, 2023, by Noah Jonathan Craft, All Rights Reserved.

This thesis is dedicated to my parents and brothers for their encouragement.

ACKNOWLEDGEMENTS

I would very much like to thank Dr. Alexander Bochdansky, my advisor and mentor during this research, for his unwavering support. I also would like to give thanks to Dr. Dreux Chappell and Dr. Rodger Harvey for their constructive feedback and the time they spent serving as members of my committee. Patrick Curry and Curtis Barnes of the RV Fay Slover, and Greg Lang – who also took the nice pictures of the algal cells – were instrumental in the collection of our mesopelagic water, and the experiments could not have been done without funding from the National Science Foundation. Lastly, I would like to show my appreciation for the professors I have studied under and/or interacted with during my time at ODU, as well as the OES department as a whole.

NOMENCLATURE

<i>D</i>	Instantaneous rate of decay, d^{-1}
<i>DPM</i>	Disintegrations per minute, ml^{-1}
<i>Q₁₀</i>	Temperature coefficient, (No Units)
<i>R</i>	Rate, (No Units)
<i>T</i>	Temperature, °C
<i>t</i>	Time, hours

TABLE OF CONTENTS

	Page
LIST OF TABLES	x
LIST OF FIGURES	xi
INTRODUCTION	1
METHODS	8
EXPERIMENTAL OVERVIEW AND CREATION OF TREATMENTS	8
CARBON FRACTION AND CELL COUNT SAMPLING PROCEDURES	11
CELL COUNT PREPARATION AND ANALYSIS	13
BIOCHEMICAL FRACTIONATION PROCEDURES	13
CARBON DECAY MODELS AND STATISTICS	15
RESULTS	17
DISCUSSION	36
CARBON ENRICHMENT	36
REPORTED DECAY RATES	38
CONSIDERATION OF LIVE CARBON	42
TRENDS IN NONLIVING TREATMENTS	44
EFFECT OF COMPOSITION ON DECAY	48
BIPHASIC DECAY	50
MEASURES OF BIOMASS	51
BIOCHEMICAL FRACTIONS	53
FUTURE CARBON CYCLING AND SUMMARY	55
CONCLUSIONS	57
REFERENCES	59
APPENDIX	77

VITA..... 80

LIST OF TABLES

Table	Page
1. Carbon degradation experiments using ^{14}C -labeled substrates.....	9
2. Estimated carbon amounts added, and DPM values measured for each treatment at the beginning and end of the experimental time frame	18
3. ANCOVA homogeneity of slope test results for comparisons of the natural log-transformed remaining POC and DOC over time between different algal species	25
3. Continued.....	26
4. Protist grazer cell count statistics for multiple algal species and carbon treatments	28
5. ANCOVA homogeneity of slope test results for comparisons of biochemical fractions over time in the POC treatments	33
6. Average decay rates for the biochemical fractions in the 12 °C live treatment and the dead POC treatments, calculated using first-order kinetics for each sample interval	34
7. Literature summary of carbon remineralization rates by particle type, and methods used	39
7. Continued.....	40
8. Time points when inflections in natural log-transformed POC data occurred, the slopes for the phases, and the difference between them for each treatment	46

LIST OF FIGURES

Figure	Page
1. Pictures and approximate sizes of the three tested algal species, from radiolabeled cultures in our laboratory	6
2. Experimental design and protocol for the live $PO^{14}C$, dead $PO^{14}C$ and $DO^{14}C$ treatments of algal-derived material in the mesopelagic experiments.....	10
3. Protocol for the biochemical fractionation of POC samples	14
4. Time series of organic carbon decay and biomass over time in the first experimental set.....	19
5. Time series of POC decay and biomass over time in the second experimental set	22
6. Time series of DOC decay and biomass over time in the second experimental set	23
7. ATP values plotted against prokaryote abundances from the nonliving (POC and DOC) treatments	30
8. Biochemical fractionations of POC samples taken from one live and several dead POC treatments, at three time points during the experimental time frames	31
9. Horizontal bar chart of carbon remineralization rates calculated in previous studies, and our regression slope data separated by phase and carbon treatment.....	41

INTRODUCTION

Globally, an average of ~10% of primary production is exported out of the euphotic zone in the form of sinking particles (such as marine snow aggregates and fecal matter) (Wakeham and Lee, 1993). Most of the particulate organic matter (POM) is remineralized through zooplankton and microbial processes (Wakeham and Lee, 1993; Steinberg, 2008; Siegel et al., 2016). Particulate matter decays according to the Martin curve, as a result of bacterial and zooplankton activity. Bacteria use extracellular enzymes to degrade organic matter while zooplankton engage in fragmentation, feeding and active transport (Steinberg, 2008). It is estimated that bacteria are responsible for the majority of the organic decay (Karl et al., 1988; Giering et al., 2014). However, zooplankton and fish – especially those undergoing migration – contribute substantially to the decay and repackaging of POC in the mesopelagic zone (Saba et al., 2021). This contribution, though, is much harder to quantify. A very small fraction of the initial organic matter makes it through the mesopelagic zone’s sequestration depth (200-1000 m) (Lee et al., 2004; Passow and Carlson, 2012; Giering et al., 2014). Carbon sources that sink through the water column experience disaggregation, dissolution, and degradation by microbes, and less than 1% (by weight) remains by the time they reach the sediment of the average seafloor depth (Lee et al., 1998; Omand et al., 2020). Organic matter decay can be simply described with the equation $\text{CH}_2\text{O} + \text{O}_2 \rightarrow \text{CO}_2 + \text{H}_2\text{O}$, a reaction in which oxygen is used to degrade organic matter and form carbon dioxide and water (Kirchman, 2018). The net vertical transfer of carbon is the so-called “biological pump,” the process that describes the movement of carbon from the ocean’s surface layer to deeper within the water column where it undergoes partial mineralization (Ducklow et al., 2001; Hansell, 2009; Jiao et al., 2010). The biological pump is

essential for the transformation and sequestration of anthropogenic carbon in the ocean, the balance of nutrient input and primary production in the euphotic zone, and sustenance for deep-ocean organisms (Siegel et al., 2023; Gooday, 2002).

The rate of decay associated with organic material in the mesopelagic layer is a critical parameter in ocean models, necessary to better predict the amount of carbon sequestered in the deep sea. Most emphasis in previous research has been on factors regulating photosynthesis and net primary production limited to the upper ocean; however, microbial solubilization and remineralization rates are factors that are similarly important for inclusion in biological pump models. The mesopelagic zone is of great importance to the marine carbon cycle because of the extent of remineralization that occurs there (Tréguer et al., 2003). Despite the numerous studies that have been done purely in laboratory conditions, few have been conducted *in situ* or with microbes collected *in situ* from mesopelagic habitats, and the estimates have ranged widely for those that have. There remains fundamental questions that need to be answered, such as whether the type of organic material subjected to decay has an influence on the rate of decay it undergoes.

Organic matter can be separated into its particulate and dissolved fractions. The difference between particulate organic matter (POM) and dissolved organic matter (DOM) lies in the size of the particles, the cutoff for which is usually a filter pore size of 0.2 to 0.7 μm , but is not consistent across all literature (e.g., Nagata, 2008; Cabrera-Brufau et al., 2021). POM is made up of both living and nonliving material, while the composition of DOM consists of colloids in addition to particles smaller than the cutoff size (Nagata, 2008). The rate of remineralization associated with sinking POM is dependent on the speed at which it is sinking, while the movement of DOM is restrained to water masses (Tréguer et al., 2003). Therefore, the composition of organic matter will determine its sinking velocity and where in the water column

the organic matter will serve as a source of carbon and nutrients to the local bacterial community (Tréguer et al., 2003; Nagata, 2008).

Particulate organic carbon is made up of organic matter from phytoplankton, bacteria, fecal pellets and cell/organismal debris, in addition to inorganic matter (Fang et al., 2015). The main emphasis on particulate organic carbon (POC) in previous research, whether live or dead, is based on the fact that microbial organisms that live in the deep sea receive most of their carbon and energy through the solubilization of particulate rather than dissolved organic matter (Bergauer et al., 2017). Not all of the POC that reaches the mesopelagic zone is rapidly degraded, as 10% has been found to escape remineralization in the upper region of the mesopelagic zone (>220 m) (Kheireddine et al., 2020). However, greater knowledge of POC fluxes and particle remineralization at depth is required to better constrain future marine carbon estimates and to more accurately predict POC export (Henson et al., 2022).

Sinking particles composed of organic matter bring not only particulate organic carbon, but also trapped dissolved organic carbon (DOC) into the bathypelagic zone as they sink (Lopez et al., 2020). Under these circumstances, relatively fresh DOC can make it into the deep sea. Conversely, the much slower subduction of DOC with slow-moving ocean currents mostly delivers refractory or semi-labile DOC to the bathypelagic environment (Carlson et al., 2010; Hansell, 2013).

Most marine DOM comes from autotrophic plankton at the ocean surface (Hansell et al., 2009). DOM is released by phytoplankton processes in addition to viral lysis and predation (Kirchman, 2018). Ocean overturning (e.g., via thermohaline convection and seasonal deep mixing) results in the export of DOC to depth (Ducklow et al., 2001; Tian et al., 2003; Hansell et al., 2009). In the deep ocean, DOC is made up of both semi-labile and refractory fractions, which

differ in their reactivity and residence time: the former fraction takes a minimum of one year and a maximum of decades to be removed from the oceanic reservoir, while the latter fraction takes thousands of years to decay (Hansell et al., 2009). A model by Hansell et al. (2009) estimates that one fifth of the total carbon associated with global ocean export production (i.e., 1.8 Pg C yr^{-1}) is in the form of semi-labile DOC that is involved in net export below 100 m in depth. The main role of DOC is to fuel bacterial production (Kirchman, 2018). There are two known sources of DOC in the mesopelagic zone that are presently not well constrained. One such source is the fraction of DOC associated with fecal pellets and ballasted marine snow particles (i.e., fast-sinking particles) (Alldredge, 2000). Another source relates to POC that is solubilized as a result of zooplankton feeding and microbial decay processes (Alldredge, 2000; Møller et al., 2003; Robinson et al., 2010).

Live or at least undecayed phytoplankton have also been known to make it to the bottom of the deep sea in the form of dense aggregates (Billett et al., 1983; Lampitt, 1985; Beaulieu, 2002; Nodder, 2007; Glover et al., 2010; Karl et al., 2012; Conte and Weber 2014). Fresh/healthy phytoplankton, especially diatoms, are known to make it to great depths of even up to 4,000 m (Agusti et al., 2015). Liu et al. (2022) found intact dead diatoms in addition to chrysophytes and dinoflagellates in the mesopelagic and below. The diatoms had relative abundances of >80% of the total three groups in the water column and the remaining <20% belonged to the other two groups (Liu et al., 2022). Chlorophyta have been identified in the mesopelagic zone at depths of 200 and 500 m, although at very low abundances compared to other sampled communities of pico-/nano-phytoplankton (Guo et al., 2018). Therefore, the flux of intact or even live cells must be accounted for, especially as they represent a source of fresh undegraded material.

Here we are only concerned with the microbially-driven degradation rates in mesopelagic waters. Many carbon-specific remineralization rates have been obtained in past studies, though they vary greatly depending on the experimental conditions. Previous decay rates vary from $\sim 3 \times 10^{-5}$ to $>0.2 \text{ d}^{-1}$, with some values even greater than 1 day^{-1} (e.g., Seiki et al., 1991; Harvey et al., 1995; Cavan et al., 2017; Lønborg et al., 2018; Cavan and Boyd, 2018; Cabrera-Brufau et al., 2021). The contribution of differences in substrate and in microbial communities to the variation in the observed decay rates is still poorly understood. Size-scaling of the amounts of protein, lipids and carbohydrates in algal species is believed to affect the nutrition they provide through predation and the carbon biogeochemical cycle (Finkel et al., 2016). However, prior research suggests that the size of a given phytoplankton cell exerts more control than phylogeny over how protein and lipid content, in addition to energy, vary (Finkel et al., 2016).

The objective of this research was to study the degradation of organic matter, both particulate and dissolved, by a microbial community collected from the mesopelagic zone in the North Atlantic Ocean. These experiments were designed to better understand the specifics of carbon degradation involved with different forms of organic matter at low temperatures like those seen in the mesopelagic zone, and the microbial populations present at that depth (~ 300 m). Among the forms of organic carbon presented in our experiments were live cells, POC and DOC from the diatom *Thalassiosira weissflogii*, in addition to POC and DOC derived from two other species of algae: a non-calcifying strain of the coccolithophorid *Emiliana huxleyi* and the chlorophyte *Tetraselmis* sp. (Fig. 1). The algal species were presented to the same mesopelagic microbial community in parallel incubations. We hypothesized that the carbon fraction and the substrate's state of life would exercise greater control over decay kinetics than the algal species, due to differences in decay between POC and DOC and live phytoplankton cells' capability to



E. huxleyi

T. weissflogii

Tetraselmis sp.

Fig. 1. Pictures and approximate sizes of the three tested algal species, from radiolabeled cultures in our laboratory.

resist degradation. Therefore, we predicted that DOC decay would be more rapid than POC decay, and live treatments would decay more slowly than dead treatments.

METHODS

EXPERIMENTAL OVERVIEW AND CREATION OF TREATMENTS

Table 1 lists the specifics of the multiple mesopelagic collection experiments and the algal treatments. The first experiment tested live cells from one algal species, the second tested live cells and nonliving organic matter from one species and the third tested nonliving organic matter from three species (Table 1). In each experiment at least one treatment was kept the same so that direct comparisons were possible, as mesopelagic water was collected at different times of the year and could therefore include different microbial communities (Table 1). The number of treatments was limited by the amount of algal culture material and mesopelagic water (Table 1). To simulate decay, we used model material (live cells, POC and DOC) in a state in which they could be easily homogenized for subsampling in a time series, and at low enough concentrations that the additions of organic material would not be overwhelming or deplete the water too much of oxygen. Carbon-14-labeled algal cultures (*E. huxleyi*, *T. weissflogii* or *Tetraselmis* sp.) in the early stationary phases were first gently filtered onto 0.8 μm polycarbonate filters (Isopore) and then resuspended in 0.2 μm filtered artificial seawater in order to remove any remaining inorganic ^{14}C . The resuspended cells were then frozen at $-80\text{ }^{\circ}\text{C}$ for at least one hour to kill the cells and break them up to release DOC. Before the experiments, a sample of the culture was vacuum filtered through a 0.2 μm filter, an operational cutoff for the separation of POC and DOC (as in Cabrera-Brufau et al., 2021). The PO^{14}C fraction remained on the filter while the DO^{14}C fraction became the filtrate (Fig. 2). The algal material on the filter was then resuspended in the original volume of water. DOC in our experiments thus represents cell lysates, which better approximate the destruction of cells by viral lysis or zooplankton feeding, instead of exudates which would grow different types of communities (Kieft et al.,

Table 1Carbon degradation experiments using ^{14}C -labeled substrates.

Experiment	Date	Water	Substrate	Incubation temperature	Treatments
1	October – December 2020	Mesopelagic	<i>T. weissflogii</i>	8 °C	Live cells
2	Late May – August 2021	Mesopelagic	<i>T. weissflogii</i>	12 °C	Live cells, POC & DOC
3	March – June 2022	Mesopelagic	(1) <i>T. weissflogii</i> (2) <i>E. huxleyi</i> (3) <i>Tetraselmis</i> sp.	12 °C	(1) POC (2) POC & DOC (3) POC & DOC

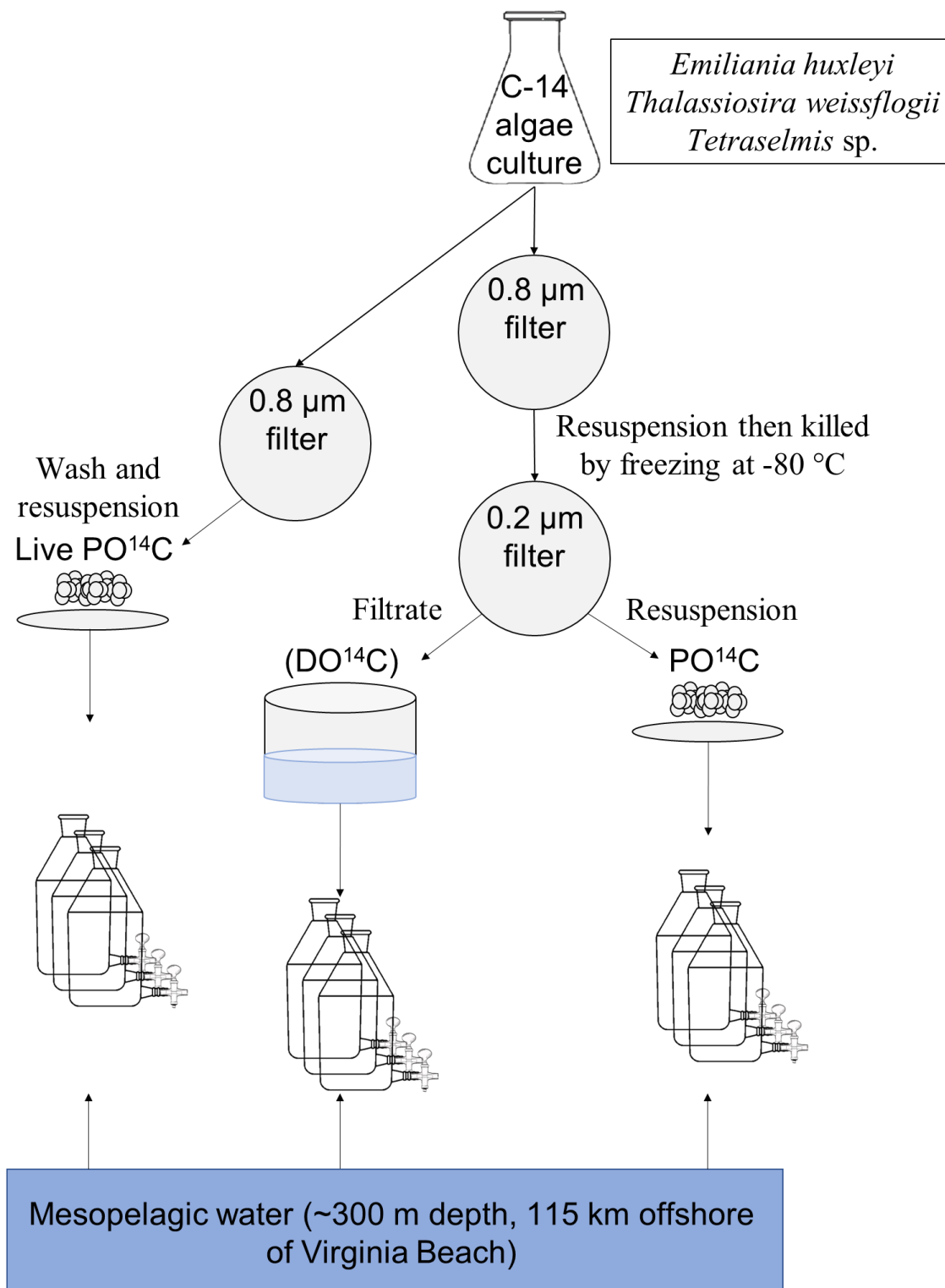


Fig. 2. Experimental design and protocol for the live $PO^{14}C$, dead $PO^{14}C$ and $DO^{14}C$ treatments of algal-derived material in the mesopelagic experiments. All incubations were performed in triplicates.

2021). For the live treatments, *T. weissflogii* cultures were filtered (using 0.8 μm filters) then washed and resuspended in unlabeled seawater, and added to the experimental carboys immediately without further treatment.

The mesopelagic water was collected from a depth of 300 meters, 115 km offshore of Virginia Beach (36.788° N, 74.629° W) using four 5-L Niskin bottles. The water temperature at the depth of collection was consistently 12 ± 0.5 °C, regardless of season. The water was gently transferred from the Niskin bottles through a hose into two 20-L bladder tanks which were immediately placed into a temperature-controlled cooler at either 8 °C (experiment 1) or 12 °C (experiments 2 and 3) (Table 1). Air bubbles were kept at a minimum during transfer. Upon arrival to the lab, and on the same day of collection, the water was moved to a dark temperature-controlled room in which the experiments were performed and also set to the same temperature (8 or 12 °C). The experiments began a day after collection. Thirteen ml of either the live algal suspension, PO^{14}C , or DO^{14}C were added each to 1.7 L of mesopelagic water in 4-L aspirator flasks. Samples were taken through a tube and a plastic ball valve connected to the aspirator flask to measure PO^{14}C , DO^{14}C , ATP, and prokaryote abundance, and for biochemical fractionation.

CARBON FRACTION AND CELL COUNT SAMPLING PROCEDURES

Before sampling at each time point, the water in the flasks was swirled until well mixed. From each flask, 10-30 ml of water was purged, and then 30-40 ml was collected into 50 ml Falcon centrifuge tubes. The protocol for the sampling of the carbon fractions was as described in Bochsansky et al. (2010). From the collected water, four 5 ml samples were immediately vacuum filtered onto GF/F filters. The first three filters were placed into plastic pony vials for PO^{14}C analysis. The fourth filter (for ATP) was placed into a cryovial that contained 1 ml of

phosphoric acid-benzalkonium chloride (P-BAC) extractant, left at room temperature for 20-30 minutes for extraction, and afterwards kept in a -80 °C freezer until analysis (Bochdansky et al., 2021). Three 0.5 ml allotments of the filtrate were placed into separate pony vials for analysis of the DO¹⁴C fraction. The vials containing the POC and DOC fractions were acidified with 0.250 ml of 0.2 N perchloric acid to eliminate remaining label, and left overnight (Bochdansky et al., 2010). Scintillation cocktail was added to the vials the next day, which were then capped, inverted to ensure homogeneity, and analyzed on a liquid scintillation counter (LSC) (Perkin Elmer Tri-Carb model 3110) using a 20 minute count setting per vial (to ensure sufficient time to get accurate readings). Three blanks with only scintillation cocktail were run every other time point, their values averaged and subtracted from the sample values. The remainder of the liquid samples kept in the Falcon tubes were fixed for cell counts. Buffered 37% formaldehyde was passed through a 0.2 µm filter and then added to each sample at a final concentration of 0.2% and left overnight. The next day, subsamples of 5 ml were filtered onto black polycarbonate membranes (Isopore GTBP) and stored in a -80 °C freezer until analysis under the epifluorescence microscope. Depending on the experiment, one or two filters were prepared for each flask at each time point.

The analysis of ATP samples followed the procedure of Bochdansky et al. (2021), which was modified from Holm-Hansen and Booth (1966). From each cryovial, 10 µl of sample was placed into triplicate scintillation vials along with 3 ml of ~18.2 MΩ ultrapure water (Barnstaed) and 50 µl of CellTiter-Glo 2.0 (Promega, protocol modified as in Bochdansky et al., 2021). A standard solution, made with 50 µl of an ATP standard of 16.4 nM concentration, was added along with the sample, water and CellTiter-Glo to a fourth vial (Bochdansky et al., 2021). The standards were interspersed with the samples during counting on the LSC to track the slow (i.e.,

over many hours) decay in luminescence over time, which allowed for a precise calculation of the ATP values.

CELL COUNT PREPARATION AND ANALYSIS

Prokaryote cell count samples were thawed and desiccated before analysis to avoid condensation on the slides. The membranes were embedded in a mounting medium that contained 4',6-diamidino-2-phenylindole dihydrochloride (Fluoroshield with DAPI, F6057, Sigma-Aldrich) to make the double-stranded DNA fluoresce (Porter and Feig, 1980). Immersion oil was added on top of the cover slips before the prokaryote cells were counted using an Olympus BX51 epifluorescence microscope at 2000x total magnification (Hobbie et al., 1977; Porter and Feig, 1980; Taylor et al., 2003). Vertical and horizontal sections (15 smaller fields for prokaryotes and 30 full fields of view for protist grazers) were counted for each section, then averaged and converted to per ml counts. Protist grazers were identified by their conspicuous nuclei that were larger than the prokaryotes. Counter staining with fluorescein isothiocyanate (FITC, Millipore Sigma) and CellMask (Invitrogen) to visualize the entire cell body instead of just the nucleus did not improve the protist grazer counts, and these efforts were discontinued in favor of a more expedient count using DAPI only.

BIOCHEMICAL FRACTIONATION PROCEDURES

At three time points during the experiment (i.e., the beginning, middle and end), samples were taken from each flask for biochemical analysis. Approximately 100 ml of liquid sample per flask was filtered through a GF/F filter, which was then frozen at -80 °C until biochemical fractionation of the samples was conducted. The fractionation process is described in Garrison and Bochkansky (2015), based on the protocol by Li et al. (1980) and later modified by Rivkin (1985) (Fig. 3). Briefly, lipids were extracted and separated from the low molecular weight

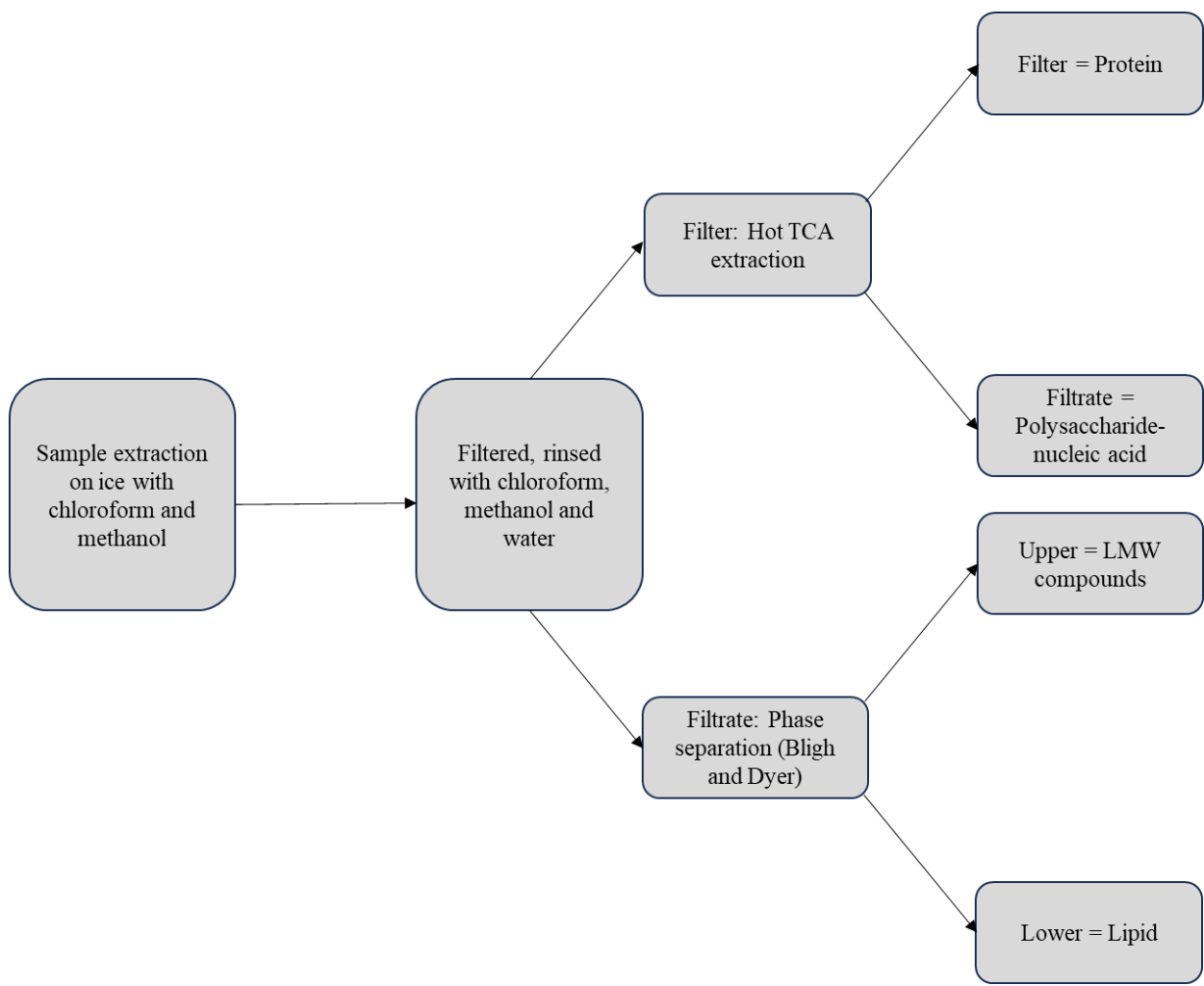


Fig. 3. Protocol for the biochemical fractionation of POC samples. Modified from Fig. 2 in Danna Palladino’s MS thesis (ODU, 2010).

fraction through chloroform, methanol and water separation (i.e., the Bligh and Dyer protocol) (Fig. 3) (Garrison and Bochdansky, 2015). Polysaccharides-nucleic acid fractions (poly-NA) and proteins were separated by division into a 5% hot TCA-soluble (poly-NA) and hot TCA-insoluble (protein) fractions (Fig. 3) (Garrison and Bochdansky, 2015). Scintillation cocktail was added to each fraction and counted using the LSC. To produce the ternary plots, the percentage of each constituent was calculated by taking the sum of the protein, lipid and poly-NA fractions only, and dividing each fraction by the sum of the whole. Decay rates were calculated for each of the four fractions using first-order kinetics over the two time intervals.

CARBON DECAY MODELS AND STATISTICS

We identified early on that the trajectory of carbon decay over time visually appeared to consist of at least two separate phases. Piecewise regressions were used with the natural log-transformed percentages of remaining $PO^{14}C$ and $DO^{14}C$ over time to find a break point at which to separate the model into two distinct phases. Where the regression algorithms did not converge, we manually selected the break points to maintain consistency among treatments. In the live treatments, the onsets of mass cell mortality changed the slopes drastically, so we made these and the two adjacent time points for each treatment the first phases of decay. We calculated exponential decay rate constants for each phase, using linear trendlines with the natural log-transformed data. Analysis of Covariance (ANCOVA) homogeneity of slope statistical tests were used on natural log-transformed values to assess significance between treatments, variables, and biochemical fractions. The DPM values of $PO^{14}C$ and $DO^{14}C$ samples were also used to calculate first-order kinetics for each pair of time points when samples were taken (Eq. 1). The first-order kinetics equation is described by:

$$D = \ln(dpm_{t1}/dpm_{t2}) (t_2-t_1)^{-1}, \quad (1)$$

where D is the instantaneous rate of decay (d^{-1}), dpm_{t_1} and dpm_{t_2} the initial and final values, respectively, of ^{14}C in the POC or DOC fractions, and t_1 and t_2 the time points of the paired samples (d).

We also compared our two biomass indicators, ATP and prokaryote abundance, against each other to identify any correlation between the variables. We plotted a linear regression with our measured values and another linear regression based on predicted ATP values that were calculated from estimates of 20 fg cell^{-1} (Lee and Fuhrman, 1987) and a mass conversion coefficient of 250 for carbon and ATP (Holm-Hansen, 1969).

RESULTS

The live, POC and DOC treatments were created from uniformly ^{14}C -labeled algal cultures. Therefore, the relative disintegrations per minute (DPM) values reflect the relative amount of carbon in each of the treatments. Table 2 shows the average DPM values at the beginning and end of each treatment's experimental time frame, in addition to the estimates of carbon added to every carboy in each treatment (see Discussion for details on which the approximate carbon estimates are based). The POC and DOC treatments for *E. huxleyi*, *T. weissflogii* and *Tetraselmis* sp. were split approximately 2:1, 4:1 and 5:1 in DPM, respectively, after the fractions were separated via 0.2 μm filtration (Table 2). The highest overall DPM values were found in the live *T. weissflogii* treatment, the *T. weissflogii* POC treatments, and the *Tetraselmis* sp. POC treatment (Table 2). The *E. huxleyi* POC treatment and the DOC treatments displayed lower initial and final DPM values (Table 2).

Fig. 4 displays the results from the first experimental set, which consists of the two live *T. weissflogii* treatments (one at 8 °C and the other at 12 °C) as well as the dead *T. weissflogii* POC and DOC treatments (both at 12 °C). The top two rows show two different measures of the carbon decay rates (Figs. 4a-h). The regression models in the first row are based on the natural log-transformed percentages of POC/DOC over time, which show the broad patterns of decay split into two phases (or potentially three for the live treatments) (Figs. 4a-d). In these models a straight line signifies first-order kinetics which are indicative of an exponential decay function (Figs. 4a-d). The slopes of these regression lines represent the exponential decay rate constants (unit: d^{-1}). The DOC treatment experienced the most rapid decay, followed by the dead POC

Table 2

Estimated carbon amounts added, and DPM values measured for each treatment at the beginning and end of the experimental time frame. Carbon amounts are based on a mass spectrometer reading of a live *T. weissflogii* culture, scaled to each treatment according to the DPM values.

Treatment	Fraction	Average initial DPM (ml ⁻¹)	Estimated carbon added (μg C ml ⁻¹)	Average final DPM (ml ⁻¹)	Remaining DPM (%)
<i>T. weissflogii</i> live (8 °C)	POC	2890.79	1.04	528.92	18.30
<i>T. weissflogii</i> live (12 °C)	POC	2075.81	0.75	163.39	7.87
<i>T. weissflogii</i> POC (#1)	POC	1389.79	0.50	198.88	14.31
<i>T. weissflogii</i> DOC	DOC	334.06	0.12	43.15	12.92
<i>E. huxleyi</i> POC	POC	560.61	0.20	43.01	7.67
<i>T. weissflogii</i> POC (#2)	POC	1241.21	0.45	147.43	11.88
<i>Tetraselmis</i> sp. POC	POC	1105.39	0.40	168.96	15.29
<i>E. huxleyi</i> DOC	DOC	277.07	0.10	51.04	18.42
<i>Tetraselmis</i> sp. DOC	DOC	196.71	0.07	27.92	14.19

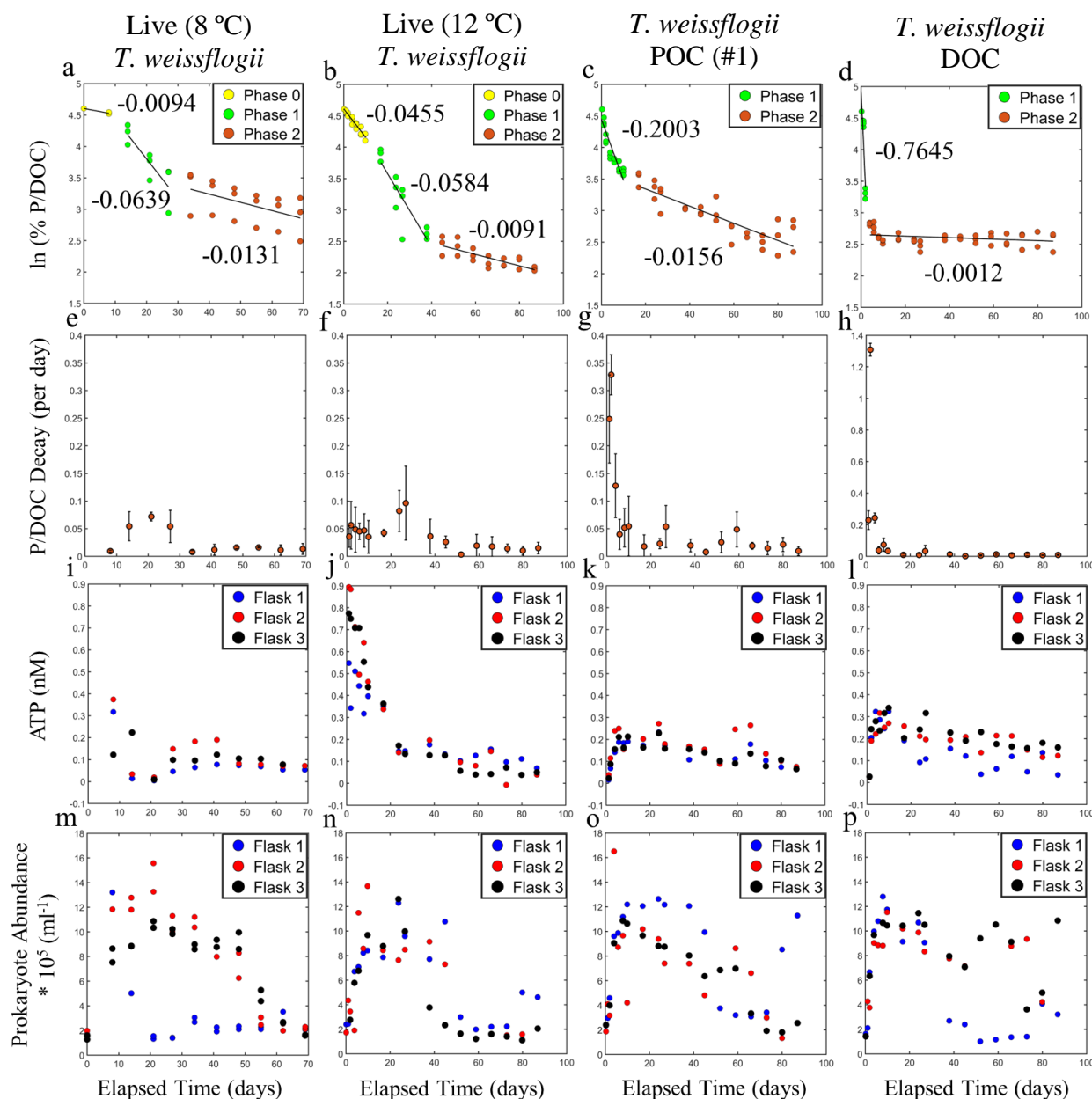


Fig. 4. Time series of organic carbon decay and biomass over time in the first experimental set. Column one (a, e, i, m) shows data from the 2020 live *T. weissflogii* treatment incubated at 8 °C, and columns two through four show data from the 2021 *T. weissflogii* experiment's live, POC and DOC treatments, respectively (incubated at 12 °C). **(a-d):** Natural log-transformed percentages of POC/DOC over time as a function of the initial DPM amount. Numbers in the panels indicate the slopes (i.e., the exponents of the exponential decay function). The r^2 values for the first and second phases of each listed dead treatment are 0.8466 and 0.7442, and 0.8519 and 0.0942, respectively. For the live treatments (8 °C and 12 °C), the r^2 values for the three phases are 0.9574, 0.7054, 0.2746, and 0.9355, 0.7761, 0.6192, respectively. **(e-h):** Average POC/DOC decay rates calculated using first-order kinetics for each sample interval (equation 1). **(i-l):** ATP representative of microbial biomass (nM). **(m-p):** Prokaryote cell counts (ml^{-1}).

treatment and lastly the two live treatments (Figs. 4a-d). The live treatment models are separated into three phases, the first of which occurs before the die-off event and is a time of smaller POC decay. After the conclusion of the first phase (phase zero) that took place in the live treatments between 8 and 10 days into each respective experiment, there was the start of a fast die-off of the live diatom cells that led into the last phase of decay which had lower rates (Figs. 4a and b). The last phase of the DOC treatment had the shallowest slope of all treatments; the live and POC treatments maintained higher degrees of decay in their second phases (Figs. 4a-d).

The second row of Fig. 4 shows the second measure of decay: highly time-resolved instantaneous decay rate constants (unit: d^{-1} – calculated using Equation 1) for each pair of time points in the experiments. This approach yields a much higher resolution and demonstrates how quickly the decay rates change between time points throughout the experiments (Figs. 4e-h). The highest peak decay rate constant was found in the DOC treatment, followed by the POC treatment and lastly the two live treatments (Figs. 4e-h). The maximum decay rates for the dead POC and DOC treatments were reached on the second day of their experiments, while the live treatments took at least 20 days to reach their peak decay rates associated with the die-offs of the live algae (Figs. 4e-h).

The two methods for measuring the microbial biomass (i.e., ATP and cell counts) showed largely similar trends. However, it is important to note that in the live treatments the ATP values were initially dominated by the live diatom cells (Figs. 4i and j). Only after the death of most of the diatom cells did ATP represent the microbial biomass present in the live treatments (Figs. 4i and j). In contrast, ATP measurements in the POC and DOC treatments solely represented the microbial biomass (Figs. 4i and j). The peaks in microbial biomass occurred relatively soon after

the addition of the substrates, which was a trend observed in all treatments across all three experimental sets (Figs. 4i-p, 5g-l and 6e-h).

Fig. 5 shows the POC treatments from the second experimental set, made from *E. huxleyi*, *T. weissflogii* and *Tetraselmis* sp., respectively. The first row again displays the natural log-transformed percentages over time, and thus the broad patterns that were observed (Figs. 5a-c). The trends in the *T. weissflogii* and *Tetraselmis* sp. POC treatments were similar to those in the POC treatment from the first experimental set, as they again consisted of two general phases of decay (Figs. 5b and c). The *E. huxleyi* POC treatment showed a greater similarity between its first and second phases of decay than any other treatment (Figs. 5a-c). The low decay seen in the first phase led to a higher decay in the second phase relative to the other POC treatments (Figs. 5a-c). The trajectory of POC decay in the *E. huxleyi* model that is split into two separate phases (first slope = -0.0325 d^{-1} and second slope = -0.0272 d^{-1}) is very similar to the model that was applied over the entire data range (slope = -0.0295 d^{-1}) (represented by the solid and dashed lines, respectively) (Fig. 5a).

The peak decay shown through time-resolved rate constants for the three POC treatments were highest for *Tetraselmis* sp. and lowest for *E. huxleyi*, with *T. weissflogii* in between (Figs. 5d-f). Again, it generally took two days for the microbial community to ramp up before they reached sufficient biomass to maximize their decay rates (Figs. 5d-f). The measures of microbial biomass were once again similar in their overall patterns (Figs. 5g-l). The ATP concentrations for the *T. weissflogii* POC treatment (#2) and the *Tetraselmis* sp. POC treatment were slightly higher than those for the *E. huxleyi* POC treatment (Figs. 5g-i). The peak ATP concentrations were reached at the time of or shortly after the peak decay rates were observed (Figs. 5d-i). The prokaryote cell count data and the ATP data both had peak values at approximately the same time

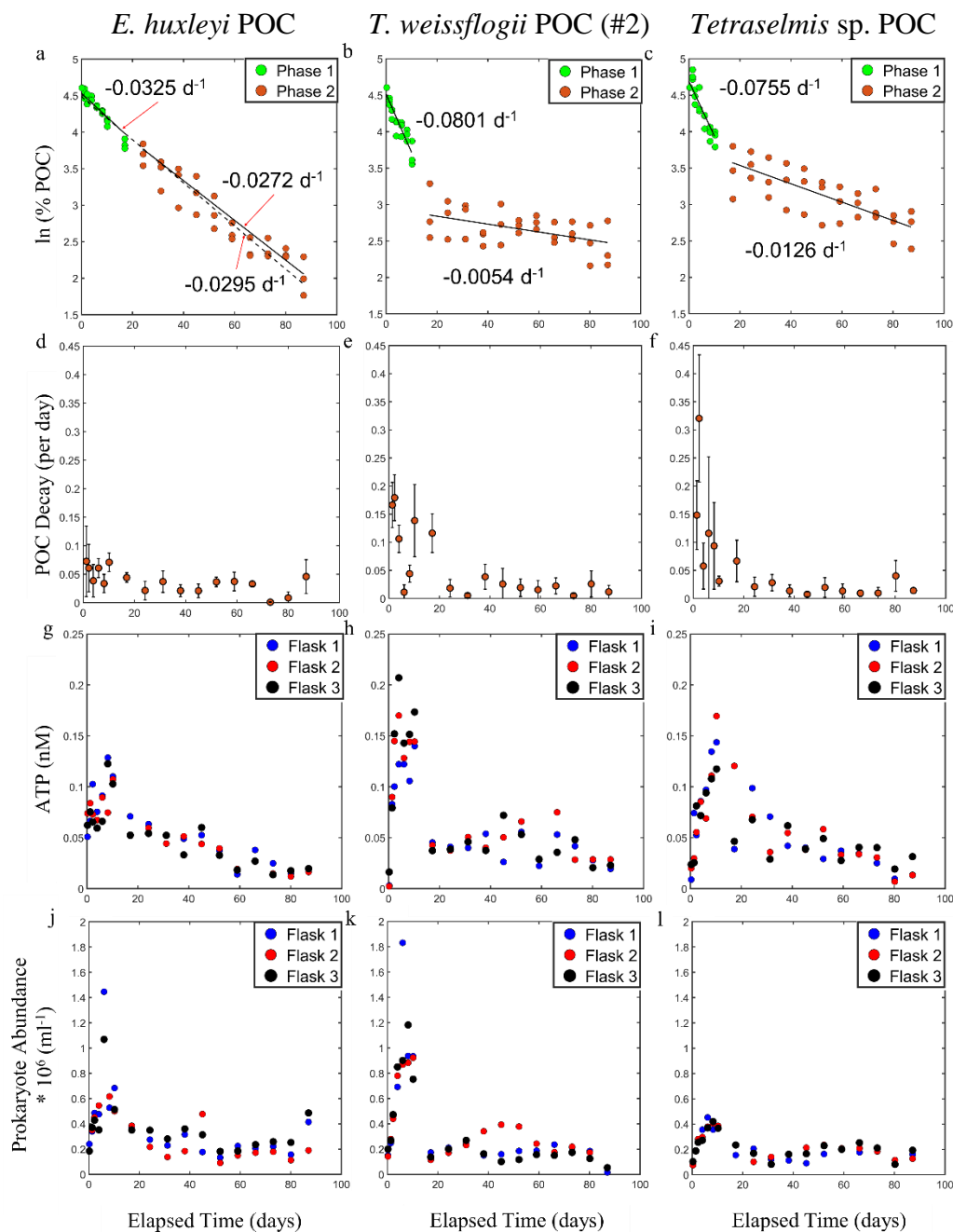


Fig. 5. Time series of POC decay and biomass over time in the second experimental set. Column one (a, d, g, j) shows data from the *E. huxleyi* POC treatment, column two *T. weissflogii* POC, and column three *Tetraselmis* sp. POC. **(a-c):** Natural log-transformed percentages of POC over time as a function of the initial DPM amount. Numbers in the panels indicate the slopes (i.e., the exponents of the exponential decay function). The r^2 values for the first and second phases of each listed treatment are 0.9600 and 0.8911, 0.8575 and 0.2502, and 0.8522 and 0.5668, respectively. The dashed line in (a) runs through the entire experimental period, and has a r^2 value of 0.9659. **(d-f):** Average POC decay rates calculated using first-order kinetics for each sample interval (equation 1). **(g-i):** ATP representative of microbial biomass (nM). **(j-l):** Prokaryote cell counts (ml^{-1}).

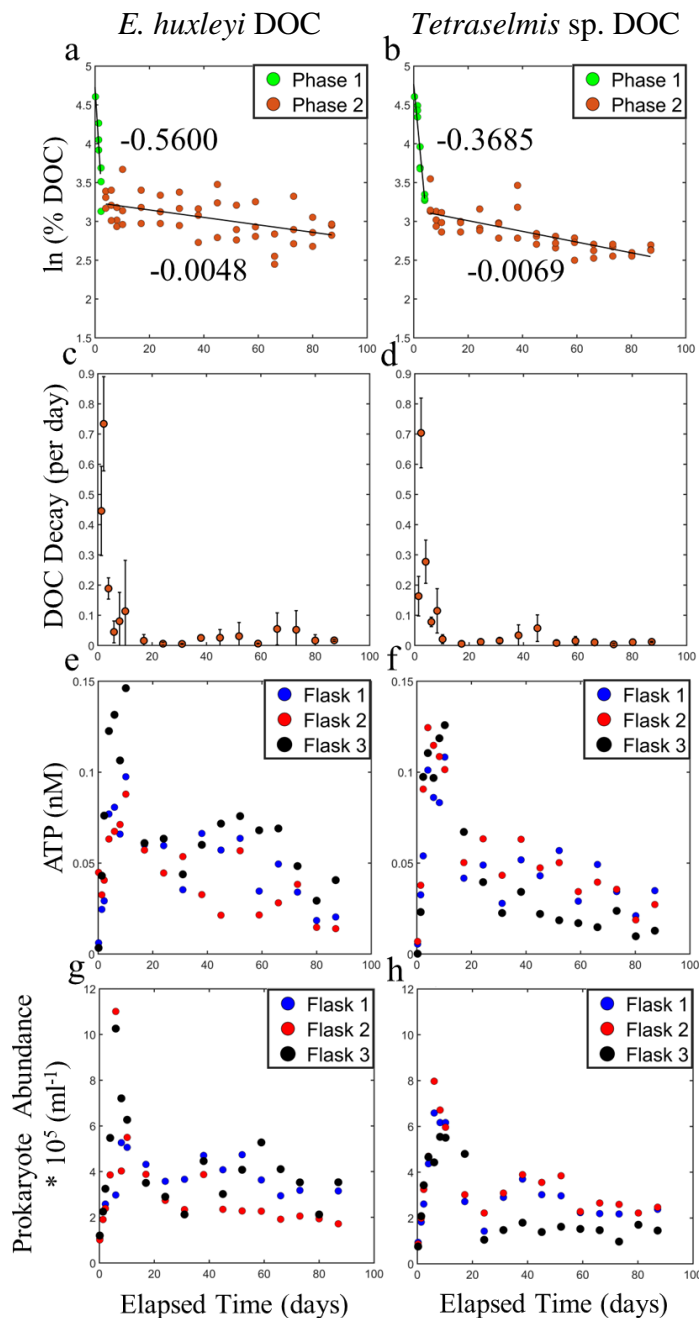


Fig. 6. Time series of DOC decay and biomass over time in the second experimental set. Column one (a, c, e, g) shows data from the *E. huxleyi* DOC treatment and column two shows data from the *Tetraselmis* sp. DOC treatment. **(a-b):** Natural log-transformed percentages of DOC over time as a function of the initial DPM amount. Numbers in the panels indicate the slopes (i.e., the exponents of the exponential decay function). The r^2 values for the first and second phases of each listed treatment are 0.8824 and 0.2720, and 0.9330 and 0.5843, respectively. **(c-d):** Average DOC decay rates calculated using first-order kinetics for each sample interval (equation 1). **(e-f):** ATP representative of microbial biomass (nM). **(g-h):** Prokaryote cell counts (ml^{-1}).

points (Figs. 5d-i). Based on cell counts, the *Tetraselmis* sp. POC treatment had a much lower peak prokaryote abundance in comparison to the other two treatments (Figs. 5j-l).

In the second set of experiments, DOC decay was only measured for *E. huxleyi* and *Tetraselmis* sp. (*T. weissflogii* DOC decay was measured in the first experimental set) (Figs. 4d, h and 6a-d). Both treatments saw very rapid decreases in natural log-transformed %DOC in the first phase that ended <10 days into the experiment. The second phases of both treatments were much shallower than the second phases of the *E. huxleyi* and *Tetraselmis* sp. POC treatments (Figs. 5a, c, 6a and b). The trends were similar to those of the *T. weissflogii* DOC treatment in the first set of experiments (Figs. 4d, 6a and b). The peak decay rate constants were similarly very high and occurred ~2 days into the experiment (Figs. 6c and d). The peak ATP values occurred around 10 days in at roughly similar concentrations (Figs. 6e and f). Both measures of biomass peaked at or soon after the peak decay rate constants (Figs. 6c-h). Generally, peak prokaryote abundances were similar across POC and DOC treatments from both experimental sets, with the exception of the lower maximum values seen in the *Tetraselmis* sp. POC treatment (Figs. 4m-p, 5j-l, 6g and h).

ANCOVA homogeneity of slopes (including randomization) tests determined that POC decay phases 0 and 1, and 1 and 2, were significantly different in the live (8 °C) treatment (Table 3). Phases 1 and 2, and 0 and 2, were significantly different in the live (12 °C) treatment (Table 3). In each of the three phases, the two live treatments were not significantly different in their POC decay over time (Table 3). The first phases of PO¹⁴C decline displayed by each algal species were significantly different from each other, but were least pronounced between *T. weissflogii* and *Tetraselmis* sp. (Table 3). The differences between algal species in PO¹⁴C decline in the second phases were also significantly different, and were most highly significant for

Table 3

ANCOVA homogeneity of slope test results for comparisons of the natural log-transformed remaining POC and DOC over time between different algal species. Also listed are p -values based on randomization tests, using 10,000 randomizations each. The p -values less than the criterion $\alpha = 0.05$ are marked with asterisks (*).

Algal species	Treatment	Phase(s)	n	ANCOVA p -value	Randomization p -value
<i>T. weissflogii</i>	Live (8 °C)	0 and 1	15	0.0269*	0.0267*
<i>T. weissflogii</i>	Live (8 °C)	1 and 2	27	0.0034*	0.0033*
<i>T. weissflogii</i>	Live (8 °C)	0 and 2	24	0.8727	0.8725
<i>T. weissflogii</i>	Live (12 °C)	0 and 1	33	0.4188	0.4147
<i>T. weissflogii</i>	Live (12 °C)	1 and 2	33	< 0.0001*	< 0.0001*
<i>T. weissflogii</i>	Live (12 °C)	0 and 2	42	0.0009*	0.0007*
<i>T. weissflogii</i>	Live (8 and 12 °C)	0	27	0.0553	0.0568
<i>T. weissflogii</i>	Live (8 and 12 °C)	1	21	0.7734	0.7754
<i>T. weissflogii</i>	Live (8 and 12 °C)	2	39	0.4132	0.4198

Table 3 Continued.

Algal species	Treatment	Phase(s)	n	ANCOVA <i>p</i> -value	Randomization <i>p</i> -value
<i>E. huxleyi</i> and <i>T. weissflogii</i>	POC	1	48	< 0.0001*	< 0.0001*
<i>T. weissflogii</i> and <i>Tetraselmis</i> sp.	POC	1	48	0.0313*	0.0295*
<i>E. huxleyi</i> and <i>Tetraselmis</i> sp.	POC	1	48	< 0.0001*	0.0001*
<i>E. huxleyi</i> and <i>T. weissflogii</i>	POC	2	60	< 0.0001*	< 0.0001*
<i>T. weissflogii</i> and <i>Tetraselmis</i> sp.	POC	2	60	0.0068*	0.0051*
<i>E. huxleyi</i> and <i>Tetraselmis</i> sp.	POC	2	60	< 0.0001*	< 0.0001*
<i>E. huxleyi</i>	POC	1 and 2	54	0.0015*	0.0015*
<i>T. weissflogii</i>	POC	1 and 2	54	< 0.0001*	< 0.0001*
<i>Tetraselmis</i> sp.	POC	1 and 2	54	< 0.0001*	< 0.0001*
<i>E. huxleyi</i> and <i>T. weissflogii</i>	DOC	1	18	0.155	0.1547
<i>T. weissflogii</i> and <i>Tetraselmis</i> sp.	DOC	1	21	0.0012*	0.0008*
<i>E. huxleyi</i> and <i>Tetraselmis</i> sp.	DOC	1	21	0.0168*	0.0187*
<i>E. huxleyi</i> and <i>T. weissflogii</i>	DOC	2	90	0.0788	0.0814
<i>T. weissflogii</i> and <i>Tetraselmis</i> sp.	DOC	2	87	< 0.0001*	< 0.0001*
<i>E. huxleyi</i> and <i>Tetraselmis</i> sp.	DOC	2	87	0.3582	0.3526
<i>E. huxleyi</i>	DOC	1 and 2	54	0.0002*	0.0001*
<i>T. weissflogii</i>	DOC	1 and 2	54	< 0.0001*	< 0.0001*
<i>Tetraselmis</i> sp.	DOC	1 and 2	54	< 0.0001*	< 0.0001*
All	Live and POC	Both	294	0.0002*	0.0002*
All	POC and DOC	Both	378	< 0.0001*	< 0.0001*
All	Live and DOC	Both	240	< 0.0001*	< 0.0001*

comparisons that included *E. huxleyi* (Table 3). The POC decline in the first versus the second phases was found to be significantly different for all species, especially for *T. weissflogii* and *Tetraselmis* sp. (Table 3). In the DOC treatments, the first phases of DOC decline were significantly different between *T. weissflogii* and *Tetraselmis* sp. and *E. huxleyi* and *Tetraselmis* sp. (Table 3). The decline in the second phases was only significantly different between *T. weissflogii* and *Tetraselmis* sp., and was highly significant (Table 3). The differences between phase one and phase two for each algal species were all highly significant (Table 3). In addition, there was high statistical significance in the differences between all live treatments, all POC treatments, and all DOC treatments when compared against each other (Table 3).

Table 4 shows data related to the protist grazer populations that were counted in each treatment from the second experimental set, just before to just after the peaks in prokaryote abundances. Counts were not done before four days, when protist grazers were exceptionally rare and therefore mostly below our detection limit. Our focus was on the abundances around the time of the prokaryote peaks and after their numbers declined to determine whether protist grazer numbers were sufficiently high to explain the fast decrease in the prokaryote populations. In addition, as cell count filters were created with only 5 ml of mesopelagic water, it was difficult to obtain accurate counts before this time. The protist grazer biomass is most relevant to determine whether they were abundant enough to cause the rapid decreases in prokaryote numbers or whether other factors were at play (e.g., viral lysis and/or resource limitation). The *Tetraselmis* sp. and *T. weissflogii* (#2) POC treatments contained the highest mean and maximum abundances of protist grazers, and the former treatment had an average abundance an order of magnitude larger than the abundances in the *E. huxleyi* and *T. weissflogii* (#2) POC treatments, and was two

Table 4

Protist grazer cell count statistics for multiple algal species and carbon treatments. Included are the approximate protist grazer abundances (\pm standard deviations) at time points close to and of the peak prokaryote abundances (days 4-24) in the experimental incubations. Also shown for each treatment is the range and the time delay between the peak abundances in prokaryotes and protist grazers.

Treatment	n	Mean abundance (ml ⁻¹)	Standard deviation	Range (ml ⁻¹)	Time since prokaryote peak (d)
<i>E. huxleyi</i> POC	14	119.35	196.27	0-705.23	11
<i>T. weissflogii</i> POC (#2)	12	498.97	775.29	0-2.26 x 10 ³	11
<i>Tetraselmis</i> sp. POC	12	1.45 x 10 ³	1.78 x 10 ³	126.94- 6.49 x 10 ³	11
<i>E. huxleyi</i> DOC	12	55.28	106.77	0-380.83	11
<i>Tetraselmis</i> sp. DOC	12	69.42	73.17	0-198.35	2

orders of magnitude larger than the abundances in the two DOC treatments (Table 4). All peaks in protist grazer abundances were reached 11 days after the peaks in prokaryote abundances, except in the *Tetraselmis* sp. DOC treatment where it occurred only two days later. The data were overall noisy but sufficient to establish that the protist grazer populations were high enough to reduce the prokaryote abundances (Table 4, see Discussion for the microbial grazing impacts). However, future experiments would be beneficial to track the development of protist grazer populations over time across treatments and species.

POC and DOC data from all nonliving treatments were combined to compare prokaryote abundances and ATP against each other (Fig. 7). The linear regression model (slope = 1.892×10^{-07}) is very close to the line predicted based on 20 fg cell^{-1} (Lee and Fuhrman, 1987) and a conversion of 250 (slope = 1.577×10^{-07}) (Holm-Hansen, 1969) (Fig. 7).

POC samples from every dead POC treatment in addition to the $12 \text{ }^{\circ}\text{C}$ live *T. weissflogii* treatment were biochemically fractionated to give bulk measurements of protein (i.e., TCA-insoluble), lipids, poly-NA (i.e., TCA-soluble) and low molecular weight (LMW) fractions. The samples contained nonspecific particulate matter, including both prokaryotes and protist grazers. The DPM values of the protein, lipids and poly-NA fractions were summed and then percentages of these three fractions (LMW excluded) were calculated to display in a ternary plot their relative changes with time over the course of the experiments (Fig. 8). The individual (i.e., not averaged) percentages are shown in Fig. S1. Samples from the DOC treatments were also fractionated to obtain biochemical information about the microbial community and any precipitates they produced but are not shown here because the sample material used in the biochemical fractionation process was performed on the filters, and not on the dissolved substrate offered as

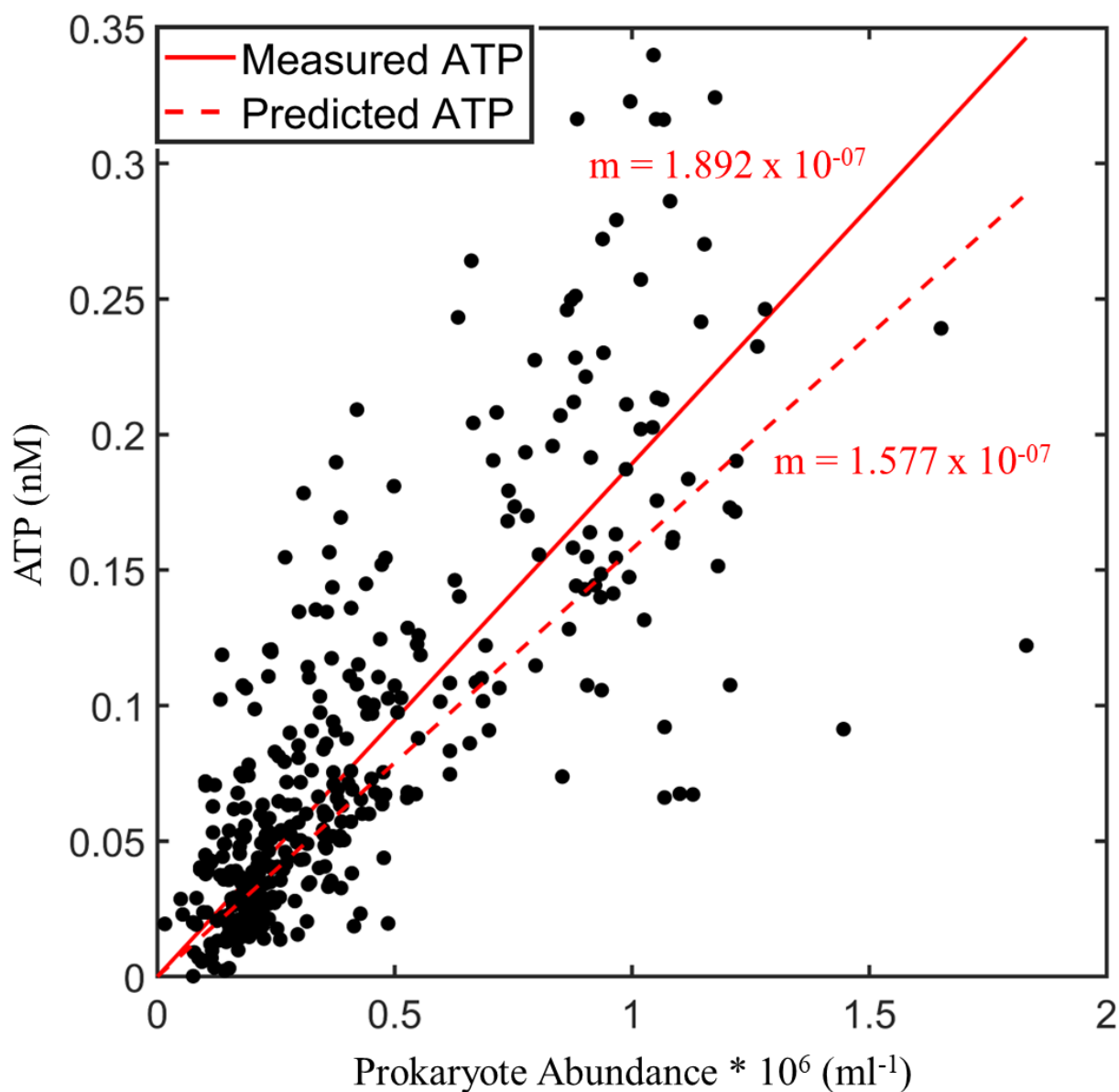


Fig. 7. ATP values plotted against prokaryote abundances from the nonliving (POC and DOC) treatments. The solid red line is a fitted linear regression ($m = 1.892 \times 10^{-07}$, $r^2 = 0.5871$, $n = 362$). The dashed line ($m = 8 \times 10^{-08}$, $r^2 = 1$, $n = 362$) represents the predicted ATP values based on prokaryote cell counts, using 20 fg cell^{-1} and a mass conversion coefficient of 250 for carbon and ATP (Holm-Hansen, 1969).

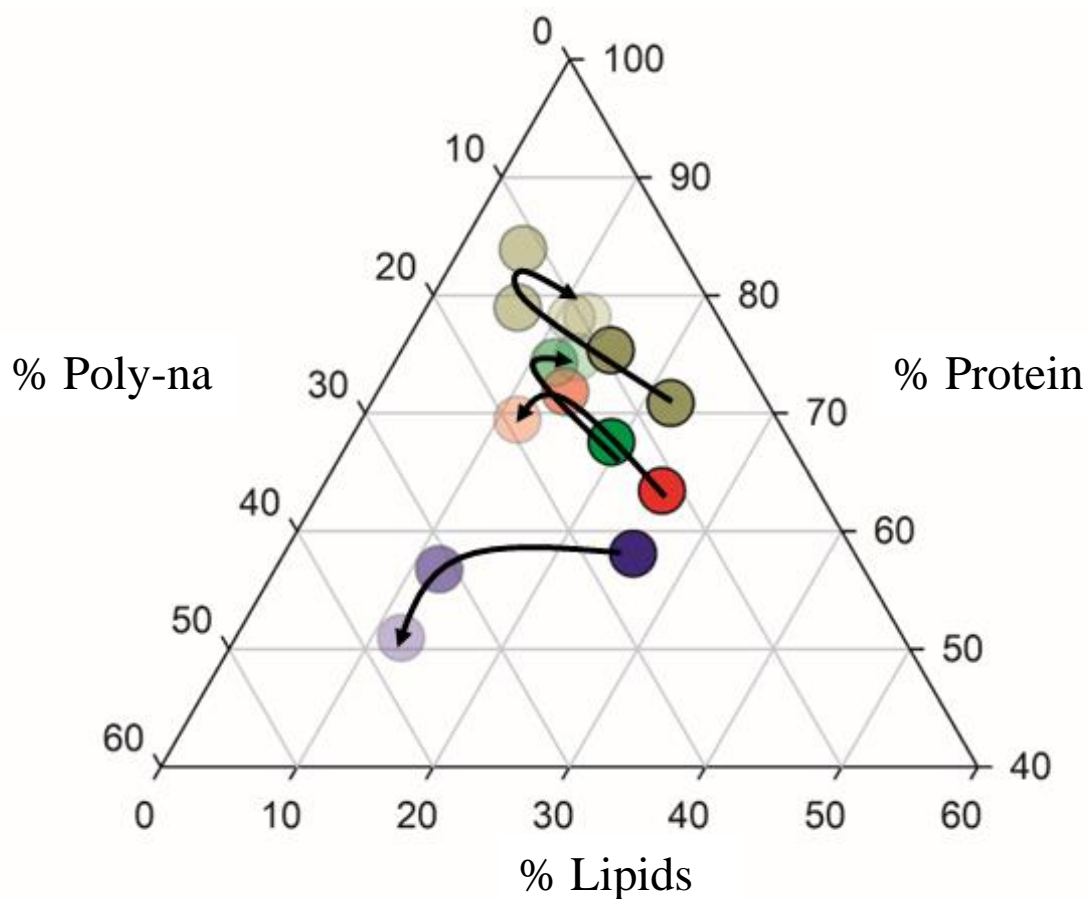


Fig. 8. Biochemical fractionations of POC samples taken from one live and several dead POC treatments, at three time points during the experimental time frames. Green represents mean values of the *T. weissflogii* live treatment, olive the *T. weissflogii* POC treatment, red the *E. huxleyi* POC treatment and violet the *Tetraselmis* sp. POC treatment. The degree of shading indicates the degree of decay, with opaque shades being undecayed and more transparent shades being more strongly decayed. Arrows represent the trajectories with time.

food (see Fig. S2). Generally, POC in these live and POC treatments had high relative percentages of protein, and decreased in % lipids and further increased in % protein over time (Fig. 8). The POC in the *Tetraselmis* sp. treatment was lower in % protein to begin with, and it decreased in % lipids and increased in % poly-NA over time (Fig. 8). The *Tetraselmis* sp. treatment deviated from the trends of the other two algae, and had a much lower percentage of protein and a higher percentage of poly-NA overall (Fig. 8). In all treatments, the changes in biochemical fractions between the first and the second time points were greater than the changes between the second and third time points indicating a much more rapid change in relative biochemical composition in the first phase of decay (Fig. 8).

The slopes of decay of the three main biochemical fractions were compared against each other for each POC treatment (*T. weissflogii* #1 and #2 data were combined) and tested for significance at $\alpha < 0.05$ using ANCOVA homogeneity of slope tests (Table 5). Differences in the percentages of protein and lipids and protein and poly-NA were significant for every algal species except for *Tetraselmis* sp. (Table 5). The differences between % lipids and % poly-NA were insignificant for each species (Table 5). Since the residuals were not normally distributed, randomization tests were performed to obtain more reliable p -values and presented along the p -values generated by MATLAB in a separate column (Tables 3 and 5) (Edgington and Onghena, 2020). In general, p -values were very similar and the randomization tests did not change whether the differences were statistically significant or not (Tables 3 and 5). Table 6 shows the biochemical fraction decay rate constants that were calculated for each treatment, which consisted of two different time intervals. In the first time interval for each treatment, the lipids fraction underwent the highest rate of decay (Table 6). However, in the second time interval lipids possessed the lowest or second lowest decay rate constants in all but the *E. huxleyi*

Table 5

ANCOVA homogeneity of slope test results for comparisons of biochemical fractions over time in the POC treatments. Also listed are p -values based on randomization tests, using 10,000 randomizations each. The p -values less than the criterion $\alpha = 0.05$ are marked with asterisks (*).

Treatment	Comparison	n	ANCOVA p -value	Randomization p -value
<i>E. huxleyi</i> POC	Protein and lipids	18	<0.0001*	0.0002*
<i>E. huxleyi</i> POC	Lipids and poly-NA	18	0.1010	0.0996
<i>E. huxleyi</i> POC	Protein and poly-NA	18	<0.0001*	0.0001*
<i>T. weissflogii</i> POC	Protein and lipids	36	<0.0001*	0.0002*
<i>T. weissflogii</i> POC	Lipids and poly-NA	36	0.1664	0.1631
<i>T. weissflogii</i> POC	Protein and poly-NA	36	<0.0001*	< 0.0001*
<i>Tetraselmis</i> sp. POC	Protein and lipids	17	0.3012	0.2989
<i>Tetraselmis</i> sp. POC	Lipids and poly-NA	17	0.4285	0.4413
<i>Tetraselmis</i> sp. POC	Protein and poly-NA	18	0.0916	0.0913
All species POC	Protein and lipids	71	0.0008*	0.0009*
All species POC	Lipids and poly-NA	71	0.1315	0.1253
All species POC	Protein and poly-NA	72	<0.0001*	0.0001*

Table 6

Average decay rates for the biochemical fractions in the 12 °C live treatment and the dead POC treatments, calculated using first-order kinetics for each sample interval.

Treatment	Biochemical fraction	Time interval 1 (d)	Average rate 1 (d ⁻¹)	n	Time interval 2 (d)	Average rate 2 (d ⁻¹)	n
Live <i>T. weissflogii</i>	Protein	22	0.0427 ± 0.0132	3	85	0.0180 ± 0.0056	3
-	Lipids	22	0.0704 ± 0.0138	3	85	0.0160 ± 0.0060	3
-	Poly-NA	22	0.0438 ± 0.0156	3	85	0.0208 ± 0.0062	3
-	LMW	22	0.0725 ± 0.0151	2	85	0.0363 ± 0.0045	2
<i>T. weissflogii</i> POC (#1)	Protein	22	0.0229 ± 0.0063	3	85	0.0131 ± 0.0025	3
-	Lipids	22	0.0831 ± 0.0058	3	85	0.0068 ± 0.0059	3
-	Poly-NA	22	0.0178 ± 0.0186	3	85	0.0159 ± 0.0058	3
-	LMW	22	0.0435 ± 0.0059	2	85	0.0069 ± 0.0037	2
<i>E. huxleyi</i> POC	Protein	9	0.0250 ± 0.0061	3	87	0.0207 ± 0.0042	3
-	Lipids	9	0.1064 ± 0.0150	3	87	0.0226 ± 0.0007	3
-	Poly-NA	9	0.0148 ± 0.0135	3	87	0.0164 ± 0.0083	3
-	LMW	9	0.0523 ± 0.0091	3	87	0.0185 ± 0.0033	3
<i>T. weissflogii</i> POC (2022)	Protein	9	0.0585 ± 0.0211	3	87	0.0106 ± 0.0079	3
-	Lipids	9	0.2026 ± 0.0266	3	87	0.0082 ± 0.0022	3
-	Poly-NA	9	0.0300 ± 0.0263	3	87	0.0139 ± 0.0111	3
-	LMW	9	0.0257 ± 0.0074	3	87	0.0188 ± 0.0029	2
<i>Tetraselmis</i> sp. POC	Protein	9	0.0998 ± 0.0318	3	87	0.0075 ± 0.0069	3
-	Lipids	9	0.1999 ± 0.0736	2	87	0.0058 ± 0.0039	2
-	Poly-NA	9	0.0427 ± 0.0127	2	87	6.5391 x 10 ⁻⁵	1
-	LMW	9	0.0080 ± 0.0003	2	87	0.0118 ± 0.0073	2

treatment (Table 6). The LMW fractions had the highest rates of decay in the second time interval for the majority of treatments (Table 6).

DISCUSSION

CARBON ENRICHMENT

Our experiments were designed to measure the degradation of marine organic matter by a natural microbial community from the mesopelagic zone. Algal cultures were used in place of marine snow particles, fecal pellets, or other substrates to ensure greater homogeneity of the subsamples taken at each time point. Samples for cell counts were taken from all radiolabeled cultures for enumeration under the epifluorescence microscope using DAPI stains, however, they were highly unreliable. *Emiliania huxleyi* nuclei were not distinguishable from bacteria in our slides, and accurate counts were therefore not possible. Diatoms were identifiable primarily due to their red autofluorescence. Their large nuclei should have been visible in the DAPI channel; however, they were either camouflaged by the silica frustules or heavily decayed so much that the actual cell enumeration was very difficult. Unlabeled cultures of *Thalassiosira weissflogii* grown under the same light and nutrient conditions on average yielded 288,000 cells ml⁻¹ in the early stationary phase, and directly-determined carbon values from a mass spectrometer averaged 137 µg carbon ml⁻¹. Dividing the amount of carbon by the cell abundance would result in a carbon per cell content of 470 pg cell⁻¹. In contrast, using the measurements shown in Fig. 1 and assuming a cylindrical shape and the conversions supplied by Menden-Deuer and Lessard (2000), the carbon content cell⁻¹ should have been closer to 51 pg per cell. This is a discrepancy of more than 9-fold, which indicates that a large amount of extracellular POC accumulated in the cultures. The carbon values of early stationary cultures were very similar among species, even in cultures of the prokaryotes *Synechococcus* and *Prochlorococcus* (unpublished values). Thus, we used the actual measurements of POC in the diatom to scale the various carbon values according to DPM values, fully acknowledging that this is only a very rough approximation. The DPM

values and conversions to carbon in the various compartments are shown in Table 2. The relatively low carbon additions added to 1.7 L of mesopelagic water – approximately between 0.75-1.04 $\mu\text{g C ml}^{-1}$ for the live treatments, 0.20-0.50 $\mu\text{g C ml}^{-1}$ for the POC treatments, and 0.07-0.12 $\mu\text{g C ml}^{-1}$ for the DOC treatments – also ensured that the composition of the treatments was more representative of mesopelagic water enriched with settling particles than of pure algal cultures. Using typical mesopelagic carbon values of 50-100 $\mu\text{g C L}^{-1}$ POC (Gardner, 1989) and 588 $\mu\text{g C L}^{-1}$ (49 μM) DOC (Vlahos et al., 2002), we therefore increased the background POC fractions approximately 3 to 21.8-fold and the background DOC fractions 1.12 to 1.20-fold in the respective treatments (Table 2). Three prior studies calculate enrichment factors (EFs – the abundance volume⁻¹ on a macroaggregate compared to the background abundance) for diatoms to be <27, between 130 and 1.7×10^3 , and between 160 and 3.9×10^3 , respectively (Silver et al., 1978; Silver et al., 1998; Alldredge, 1998; Simon et al., 2002). The EF measurements for phytoplankton sized between 2 and 20 μm are between 7 and 67 (Caron et al., 1986; Simon et al., 2002). According to previous studies, the *in-situ* enrichment factor of marine snow DOC is between 14.3 and 78 (Herndl and Peduzzi, 1988; Alldredge, 2000; Simon et al., 2002). Therefore, our carbon additions were not excessive and were well within the wide ranges of microscale variability observed in the marine environment. We expect the difference in initial DPM values between the same treatments of different algal species to be a result of different carbon amounts in each culture, which are functions of the amount of carbon per cell present in the culture of each species and the abundance of algal cells (Table 2).

Oxygen limitation was avoided during the experiments because of this relatively low input of organic material, in addition to the flasks' large surface area to atmosphere ratio and the thorough mixing before each subsample was taken. High accuracy was possible due to the high

sensitivity of the ^{14}C assay which provided sufficiently high readings for sample volumes of only 5 ml for POC and 0.5 ml for DOC, even at the end of each experiment (Table 2). A carbon mass balance (including inorganic carbon) was not possible as there was an inefficient recovery of the total dissolved carbon fraction (pre-acidification). In addition, because our carboys were open systems, losses in the dissolved inorganic carbon fraction due to the outgassing of carbon dioxide could not be prevented.

REPORTED DECAY RATES

The decay rates reported from these three experiments are net decay rates, as the carbon-14 released by the carbon treatments is partially reincorporated into the developing microbial biomass. Therefore, the C-14 of the carbon sources and that incorporated by the prokaryote community during the incubations cannot be separated from each other. The remaining carbon seen at the end of the 69 or 87-day experiments, therefore, is believed to represent both the prokaryote community and the formation of refractory material over time that can only be slowly degraded or not degraded at all. Based on our ATP values, however, the live microbial community makes up a very small fraction of carbon at the beginning of the experiment: between 0.35 and 0.83% for the POC treatments and approximately 0.17% for the DOC treatments. At the end of the 87-day period, the live microbes' fraction of carbon is approximately 3.9% for the POC treatments (5 to 11-fold increase) and 5.3% for the DOC treatments (~31-fold increase). The reincorporation of the ^{14}C label therefore had very little influence on the overall decay rate estimates.

The rates we calculated from our experiments fall within the wide ranges reported in the literature (Table 7 and Fig. 9). Most decay rates have previously been measured for particulate

Table 7

Literature summary of carbon remineralization rates by particle type, and methods used.

Particle type	Rate (d ⁻¹)	Method	Reference (by year)
DOM (Step 1)	0.01-0.09	Wet oxidation	Ogura (1975)
DOM (Step 2)	0.001-0.009	Wet oxidation	Ogura (1975)
Dried <i>Anabaena</i> cells	0.010-0.072	C-14 and quantification of released carbon dioxide	Fallon and Brock (1979)
Plankton tow	0.038	Analysis of carbon content	Westrich and Berner (1984)
Sediment trap material	0.010-0.036	Analysis of carbon content	Walsh et al. (1988)
Plankton net/sampler POM	0.044-0.232	Analysis of carbon content (dry digestion)	Seiki et al. (1991) (run 5, 5-30 °C)
Plankton net/sampler DOM	0.056-0.211	Analysis of carbon content (wet digestion)	Seiki et al. (1991) (run 5, 5-30 °C)
Diatom and cyanobacteria POC	0.035-0.053	Analysis of carbon content	Harvey et al. (1995) (oxic)
Diatom and cyanobacteria POC	0.007-0.015	Analysis of carbon content	Harvey et al. (1995) (anoxic)
Diatom aggregates	0.083	Oxygen consumption (RQ of 1.2 mol O ₂ : 1 mol CO ₂)	Ploug and Grossart (2000)
Fecal pellets	0.12	Oxygen consumption (RQ of 1 mol O ₂ : 1 mol CO ₂)	Ploug et al. (2008)
Marine snow	0.13	Oxygen consumption (RQ of 1.2 mol O ₂ : 1 mol CO ₂)	Iversen and Ploug (2010)
Diatom aggregates	0.12 (15 °C)	Oxygen consumption (RQ of 1 mol O ₂ : 1 mol CO ₂)	Iversen and Ploug (2013)
Diatom aggregates	0.034 (4 °C)	Oxygen consumption (RQ of 1 mol O ₂ : 1 mol CO ₂)	Iversen and Ploug (2013)
Fecal pellets	0.02-0.1%	Oxygen consumption (RQ not specified)	Morata and Seuthe (2014)
<i>T. weissflogii</i> cells	0.096-0.113	Analysis of carbon content	Suroy et al. (2015)
Sediment trap material	0.004-0.278	Quantification of released carbon dioxide	Collins et al. (2015)
RESPIRE sediment trap material	Undetectable–0.04	Oxygen consumption (RQ not specified)	McDonnell et al. (2015) (WAP)
RESPIRE sediment trap material	0.4-0.5 (without 1.5 outlier)	Oxygen consumption (RQ not specified)	McDonnell et al. (2015) (BATS)

Table 7 Continued.

Particle type	Rate (d ⁻¹)	Method	Reference (by year)
Diatom aggregates	0.065	Oxygen consumption (RQ of 1 mol O ₂ : 1 mol CO ₂)	Ploug and Bergkvist (2015)
Fecal pellets	0.010-0.065	Oxygen consumption (RQ of 1 mol O ₂ : 1 mol CO ₂)	Belcher et al. (2016a)
Marine snow	0.011-0.014	Oxygen consumption (RQ of 1 mol O ₂ : 1 mol CO ₂)	Belcher et al. (2016b)
Marine snow	0.35-13.7 (0.13-5 temp. corr.)	Oxygen consumption (RQ not specified) and analysis of carbon content	Cavan et al. (2017)
Humic substances DOC	0.004-0.006	Oxygen consumption (RQ not specified)	Lønborg et al. (2018) using data from Bussmann (1999)
Semi-labile DOC	0.001-0.011	Model-derived using past DOC data	Lønborg et al. (2018)
Semi-refractory DOC	3 x 10 ⁻⁵ - 7.001 x 10 ⁻⁵	Model-derived using past DOC data	Lønborg et al. (2018)
Natural heterotrophs	0.33-5.25 (0.87-1.07 in-situ temp.)	Oxygen consumption (RQ of 1 mol O ₂ : 1 mol CO ₂)	Cavan and Boyd (2018)
Suspended and sediment trap material	0.007-0.125	Oxygen consumption (RQ of 1 mol O ₂ : 1 mol CO ₂) and analysis of carbon content	Bach et al. (2019)
TOC fraction	0.22-0.37	Decarbonation	Cabrera-Brufau et al. (2021)
POC fraction	0.08-0.35	Decarbonation	Cabrera-Brufau et al. (2021)
Copepod carcasses	0.02-0.16	Oxygen consumption (RQ of 1 mol O ₂ : 1 mol CO ₂) and analysis of carbon content	Halfter et al. (2022)

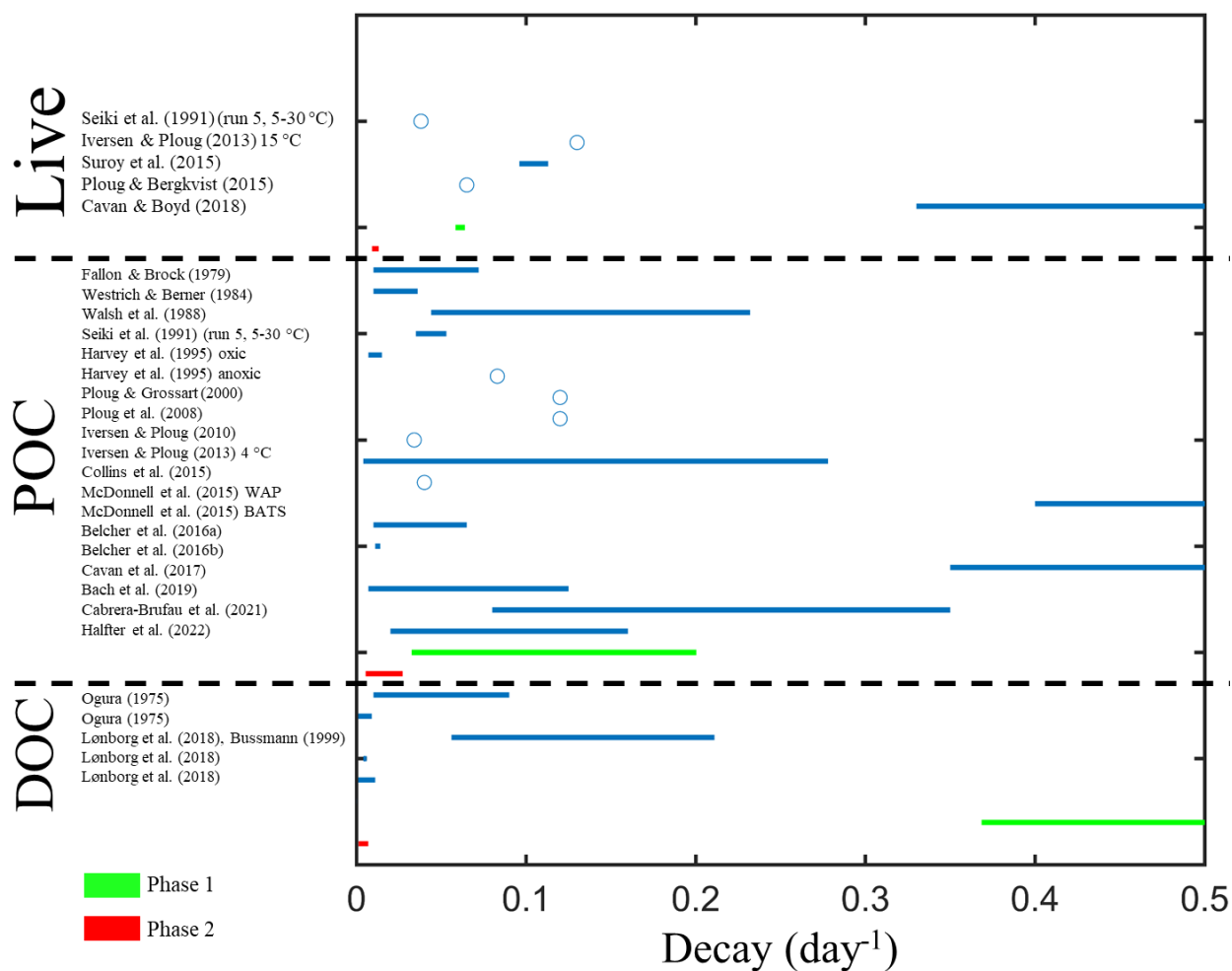


Fig. 9. Horizontal bar chart of carbon remineralization rates calculated in previous studies, and our regression slope data separated by phase and carbon treatment. Green bars represent data from phase one and red bars represent data from phase two. The authors of each study are placed next to the bars with their respective values.

sources rather than dissolved, so the upper bounds of the range of our DOC decay rates ($> 0.7 \text{ d}^{-1}$, Figs. 4h, 6c and d) are relatively unique (Table 7 and Fig. 9). The live POC decay rates ($0.003\text{-}0.096 \text{ d}^{-1}$) and the dead POC decay rates ($0.001\text{-}0.329 \text{ d}^{-1}$) fall within the ranges reported in the literature (Table 7 and Fig. 9). These rates are especially similar to those from Ogura (1975), Seiki et al. (1991), the oxic incubations in Harvey et al. (1995), Iversen and Ploug (2013), Collins et al. (2015) and Cabrera-Brufau et al. (2021). In contrast, the rates of decay reported in McDonnell et al. (2015) that measured respiration using sediment traps equipped with oxygen chambers to monitor decay (i.e., RESPIRE traps) are very high by comparison (Table 7 and Fig. 9). Most literature decay rates that are based on oxygen consumption assume a respiratory quotient (RQ) value of 1 (Table 7).

CONSIDERATION OF LIVE CARBON

There has been a long-recognized conundrum involving the relationship between the observed biological activity in the bathypelagic layer and the apparent supply of organic nutrients (Reinthal et al., 2010; Burd et al., 2010). Previous literature has suggested mechanisms that close the gap between these two variables, such as the in-situ production through yet uncharacterized production pathways (e.g., Herndl et al., 2023). Another possible mechanism is rapid, episodic sinking events that are missed by conventional calculations and steady-state assumptions, which could lead to an underestimation of the contribution of the slow-sinking particle pool (Giering et al., 2017; Smith Jr. et al., 2018). Our analysis suggests that if phytoplankton are alive while sinking, and have sufficiently rapid sinking velocities at the time of aggregate formation, they will greatly resist degradation and supply pulses of nutrients to the bathypelagic environment.

Within the live algal treatments, the trajectory of decay was best described with three phases. In the first phase (phase zero), low decay rates were present since the algae were still alive. This first phase of slower losses included the respiration of the live cells, the exudation of organic material, and likely some cell deaths. Next, a rapid die-off occurred during which POC rapidly decreased, and this was followed by a third phase of decay that was similar to the decay consistent with the dead POC treatments during the latter half of the experimental time frame (Figs. 4e-g and 5d-f). As observed with the instantaneous decay rates, POC decay began but was relatively low in the first phase, and did not peak until the diatom die-off event (phase two) (Figs. 4a and b). The rapid cell die-off released an abundance of organic material that fueled the microbial growth, as seen in the spike in prokaryote cell counts (Figs. 4m and n). Differences in decay seen in Fig. 4 and Table 3 between the 8 °C and 12 °C live *T. weissflogii* treatments can be attributed to the difference in temperature between the two incubations (8 and 12 °C) as higher temperatures cause higher rates of reactions (i.e., the Arrhenius equation) (Vallance, 2017). The 8 °C live treatment's lower incubation temperature appeared to have slowed down the decay of the organic matter in the first phase and affected both the trajectory of ATP concentrations and the response time of the microbial community. A Q_{10} temperature coefficient describes the temperature impact on a biological process (e.g., degradation) (Gillooly et al., 2001; Szewczyk et al., 2023). Using a Q_{10} of 2 (Eq. 2), and in the first phase only, much of the difference in decay rates can be explained by temperature alone. The Q_{10} equation is:

$$Q_{10} = (R_2 / R_1)^{(10 \text{ } ^\circ\text{C} / (T_2 - T_1))}, \quad (2)$$

where R_1 and R_2 are the rates at the lower and higher temperature, respectively, and T_1 and T_2 the lower and higher temperature, respectively (van 't Hoff, 1899; Hegarty, 1973; Szewczyk et al., 2023). Using this equation on the differences in decay rates of the live treatments, the actual

Q_{10} is 3.17 for the first phase. In contrast, the decay rates were very similar between the two temperatures with a Q_{10} of 0.66 in the second phase.

Using this assumption, the rates from the 8 °C experiment adjusted to 12 °C were 0.0364 for the first phase of decay and 0.0165 for the second phase. These rates were similar to the values that were measured in the 12 °C experiment (0.0438 and 0.0106 for the two phases, respectively). Both of the live treatments showed a resistance to initial decay in comparison to the POC and DOC treatments. The natural defenses associated with live algal cells, including diatoms (e.g., the production of antibiotics), and their ability to resist degradation have long been discussed in the literature (Waksman et al., 1937; Nielsen, 1955; Golueke et al., 1957; Oppenheimer and Vance, 1960). These defenses would have prevented decay until the death of those cells from their inability to perform photosynthesis and the cold temperatures. The mortality of the live diatoms accelerated between 14 and 20 days into the experiment (Figs. 4e, f, i and j). The degree of contribution of biomass to sinking fluxes is, therefore, an important but rarely measured factor in determining the transfer efficiency of the biological pump (Taylor, 1989). The resistance of live cells to decay also explains the large number of intact cells observed in the deep sea (Agusti et al., 2015; Turner, 2015; Tréguer et al., 2018; Giner et al., 2020; Zhao et al., 2022). More work needs to be done to better understand the contribution of the live carbon flux to the deep sea, but these fluxes are difficult to capture because of their highly episodic nature.

TRENDS IN NONLIVING TREATMENTS

In the non-living treatments (POC and DOC), the inflections from the first to the second phases typically occurred in the time frame of 10-24 elapsed days for the POC treatments and 2-6 elapsed days for the DOC treatments. Our results also show that the contrast between the initial

and the subsequent decay rate was more striking in experiments that used DOC rather than POC as a substrate. The easily digestible fractions in the DOC were degraded very quickly, and as with the POC treatments there were refractory (i.e., harder to digest) pools that persisted throughout the experimental time frames (Figs. 4c, d, 5a-c, 6a and b). However, the DOC treatments exhausted the easily digestible fractions much earlier on in the experiment (2-4 days in) than the POC treatments (Figs. 4c, d, 5a-c, 6a and b). After 2-4 days, the decay associated with the second phases stabilized and the slopes became notably shallow compared to the slopes in the first phases (Figs. 4d, 6a and b). It was at this point that the most labile DOC fractions had been digested by the microbial community, which left fractions that decayed very little over a period of months that would likely be classified as semi-labile (Hansell, 2013). A study by Carlson et al. (1998) on organic carbon in the Ross Sea and the Sargasso Sea concluded that the lability of the total organic carbon produced in phytoplankton blooms and its partitioning into particulate and dissolved fractions are dependent on location, and could be a result of differences in phytoplankton populations. Based on the differential decay rates we obtained from our experiments, the percentage of organic carbon that is particulate versus dissolved would control the amount of organic matter that reaches the mesopelagic zone and below. We observed a much faster and initially stronger decay of DOC than POC (Figs. 4a-h, 5a-f and 6a-d), which suggests that if both fractions were of the same age the DOC that reaches the deep sea will likely be a smaller percentage of the original quantity than the POC.

Interestingly, the decay rates in the later stages of DOC degradation were also generally much lower than the rates in the later stages of POC decay (Figs. 4g, h, 5d-f, 6c, d and Table 8). DOM naturally produced in-situ can undergo transformations into harder to digest material (Hansell, 2013). It is known that microbially-mediated remineralization can produce more

Table 8

Time points when inflections in natural log-transformed POC data occurred, the slopes for the phases, and the difference between them for each treatment. The live treatments have two points of inflection: one at the end of the first slope and one at the beginning of the third slope.

Treatment	Inflection(s) (days elapsed)	Slope 1 (-)	Slope 2 (-)	Slope 1 - slope 2 (-)
Live <i>T. weissflogii</i> #1 (8 °C)	1). 14-21 2). 21-27	0.0639	0.0131	0.0508
Live <i>T. weissflogii</i> #2 (12 °C)	1). 17-24 2). 27-38	0.0584	0.0091	0.0493
<i>T. weissflogii</i> POC #1	10-17	0.2003	0.0156	0.1847
<i>T. weissflogii</i> DOC	2-4	0.7645	0.0012	0.7633
<i>E. huxleyi</i> POC	17-24	0.0325	0.0272	0.0053
<i>T. weissflogii</i> POC #2	17-24	0.0801	0.0054	0.0747
<i>Tetraselmis</i> sp. POC	10-17	0.0755	0.0126	0.0629
<i>E. huxleyi</i> DOC	2-4	0.5600	0.0048	0.5552
<i>Tetraselmis</i> sp. DOC	4-6	0.3685	0.0069	0.3616

refractory DOM (e.g., Ogawa et al., 2001). Hansell (2013) indicated that DOC that is not degraded over a period of weeks to months probably belongs to the semi-labile fraction. Semi-labile DOC is also thought to be the DOC fraction that is the principal contributor to the biological pump, on account of the high amount exported through the water column ($\sim 1.5 \text{ Pg C year}^{-1}$) (Hansell et al., 2012; Hansell, 2013). Therefore, it reasons that the less digestible DOC fractions that formed over the course of our experiments were likely similar in nature to the fractions present in the mesopelagic. It is possible that a more diverse microbial population is required to break down the material that is harder to digest (Pedler et al., 2014).

Bacteria are believed to specialize in the type of DOC substances they preferentially incorporate from their environment (e.g., Kieft et al., 2021). For example, there is evidence that Bacteroidetes lineages have an assimilation preference for DOC from diatom lysates (Kieft et al., 2021). Pedler et al. (2014) concluded that only one bacterial strain, *Alteromonas* (AltSIO), was needed to deplete the operationally-defined labile DOC fraction. *Alteromonas* has also been found to be a common gammaproteobacterium in marine snow, with different strains thought to specialize in the colonization of larger and faster particles or smaller and slower ones (Ivars-Martinez et al., 2008). It is likely, therefore, that fresh organic material is primarily degraded by a few copiotroph specialists that can rapidly grow when given rich organic material, and then quickly fade away as a result of both depleted resources and bacterivory. Another example that shows that specialist copiotrophs may be responsible for most of the fresh carbon decay is the substantial taxonomic and functional gene differences between microbial populations growing in sediment traps, i.e., those captured in poisoned sediment traps (reflecting communities on sinking particles) and those present in the water column (Fontanez et al., 2015). Fontanez et al. (2015) found that *Alteromonas*, *Marinobacter*, *Moritella* and *Pseudoalteromonas* were the

bacterial genera found in the highest abundances in the unpoisoned traps, while *Vibrio* dominated bacterial abundances in poisoned traps.

EFFECT OF COMPOSITION ON DECAY

The decay experienced by a carbon source over time is dependent on its composition (i.e., live, dead, POC or DOC) more so than the species the organic substrates derived from. In the case of dissolved organic matter, decay processes are similarly important in the determination of the fraction of refractory DOC (Meon, 2001). Live cells resist degradation more effectively than dead material in the form of POC or DOC, and some of the early losses we observed with the live diatoms were due in part to decrease of the ^{14}C signal through cell respiration. The decay associated with POC and DOC are very different from each other in terms of the rate of decay and peak decay reached at any point of time (Figs. 4c, d, g, h, 5a-f, 6a-d and Table 8). Our data also suggest that the two phases of decay are not independent of each other. The faster decay observed in the early phases led to slower decay in the later phases (Figs. 4d, 5b, c, 6a and b). The *E. huxleyi* POC treatment began with a relatively low initial decay rate that led to a higher decay rate in the second phase than observed in the *T. weissflogii* and *Tetraselmis* sp. POC treatments (Figs. 4c and 5a-c). We cannot explain with a high degree of confidence the reason for this interrelationship, and therefore this is an area that requires further research.

We are unsure why the initial POC decay rate for *E. huxleyi* was less than that of the other two algae, but consider three possibilities. Lower decay may have been a result of the high degree of stickiness observed in the preparation of the *E. huxleyi* POC treatment. The cells were very difficult to remove and resuspend from the filter, and considerable mechanical force, including sonication, had to be used to remove the cell debris from the polycarbonate membrane. This may have mechanically solubilized material that ended up in the dissolved fraction, leading

to a slower initial decay of the retained particulate fraction. The *T. weissflogii* cells were much easier to resuspend and the *Tetraselmis* sp. cells were removed with the most ease out of the three species. The second possibility is that the presence of transparent exopolymer particles (TEP) could have slowed the decay. An increase of TEP has been previously observed on coccolithophorids in the presence of viruses (Vardi et al., 2012) and the mechanisms associated with the slower digestion of mucopolysaccharides have been observed in another haptophyte (i.e., *Phaeocystis* sp.). The low decay rate of mucus in that species is related to the high C:N and C:P ratios that possibly make it a less favorable substrate because of nutrient limitation (Alderkamp et al., 2007). Another possibility for the trajectory of the *E. huxleyi* POC treatment is that the coccolithophorid has antimicrobial protection that inhibited the growth and digestion of its matrix. However, this final possibility is unlikely given the robust growth of the microbial community, especially as reflected in the high cell counts (Fig. 5j).

Cabrera-Brufau found higher particulate organic matter decay rates in flagellate communities, largely comprised of coccolithophores and nanoflagellates, than in communities mostly made up of diatoms (Cabrera-Brufau et al., 2021). This is in contrast to our results, where at least initially the opposite was true, and diatom carbon was digested more easily (Figs. 4c, g, 5a, b, d, e and Table 8). There were, however, several main differences in the experimental protocol between our study and that of Cabrera-Brufau et al. (2021). They used conglomerations of different substrates that were not limited to individual species, and the initial incubation of the POM involved nutrient inputs and cycles of 12 hours of light followed by 12 hours of darkness. Our experiments were performed in complete darkness. Their degradation experiment was also only performed over a 19-day period (Cabrera-Brufau et al., 2021) while ours took place over 87 days.

BIPHASIC DECAY

In all of our experiments, the decrease in POC and DOC over the entire time course of up to 87 days did not follow simple first order kinetics. Viewing the data at high temporal resolutions, decay rates were complex and rapidly changing during the first few days, typically reaching peak values between 21 and 27 days for the live treatments, between 1 and 2 days for the POC treatments, and at 2 days for the DOC treatments. The rapid increase in decay rates at these times is concomitant with the rise in microbial biomass, as evidenced by both ATP measurements and prokaryote abundances (Figs. 4i-p, 5g-l and 6e-h). However, both the changes in the microbial populations and the rates of decay of the substrate are so rapid that overall, a simple model based on biphasic decay is justified when using bulk POC and DOC (Figs. 4-6). Biphasic decay was previously observed in organic matter from sediments that was studied in the laboratory, albeit on a much longer time scale (Westrich and Berner, 1984). After approximately 50 days into their experiment, the concentration of remaining POC was ~50% of the initial concentration (Westrich and Berner, 1984). Westrich and Berner (1984) suggested that the phase that extends to 50 days represents the POC fraction that is the most reactive and therefore easiest to digest. By comparison, our POC treatments at 50 elapsed days had POC percentages between 15 and 26% of the initial amount. The differences in POC decay rates could be due to differences in substrate – theirs consisted of naturally collected POC with multiple species while ours were derived from single species – and the fact that they studied benthic decay while we used pelagic microbial communities (Westrich and Berner, 1984). Digitizing the data from Westrich and Berner's (1984) laboratory experiment with Long Island Sound plankton (their Fig. 2) resulted in an instantaneous rate of decay in oxygenated water of 0.034 d^{-1} for the first phase, and 0.0004 d^{-1} for the second phase (their Fig. S1). The inflection point between these two phases was very

similar to ours, occurring 30 days after the start of the experiment with ~30% of the original POC remaining. These values are remarkably close to what we obtained in our experiments, especially in the first phase (Figs. 4c, 5a-c, 6a and b). In the water column, biphasic decay was also observed in a field study by Kheireddine et al. (2020) on a time scale more similar to ours. Their study used data collected in-situ from the Red Sea and found that over a period of a few days >85% of the exported POC that reached the mesopelagic zone underwent degradation (Kheireddine et al., 2020). In a second phase, the remainder of the exported POC took between weeks and months to degrade (Kheireddine et al., 2020). The fast initial and slow subsequent phases of decay described in Kheireddine et al. (2020) were similar to what we observed in our experiments (Figs. 4a-h, 5a-f and 6a-d). In both of these studies the authors concluded that this two-phase system is most likely a consequence of the lability of the substrate (Westrich and Berner, 1984; Kheireddine et al., 2020).

MEASURES OF BIOMASS

Biomass that contribute to the mass fluxes are not only composed of the initial phytoplankton substrates, but also of prokaryote populations and the heterotrophic protist grazers that colonize sinking aggregates. The analysis of ATP, therefore, is potentially a very useful method in determining the contribution of biomass to the overall carbon flux. From our experiments it appears that, with a few exceptions, the peak biomass typically occurs 4-10 days into the experiments. This range in time is around when particles with sinking velocities of 40-100 m d⁻¹ (Giering et al., 2017; Iversen and Lampitt, 2020) would have transited a good portion of the mesopelagic zone – i.e., 280 to 1400 m, respectively. The possibility for aggregates to sink faster than this range means that even greater amounts of live and entirely undegraded material reach the bathypelagic environment. The comparison between ATP and prokaryote counts

indicates that ATP is effective at representing live biomass, both of the initial live carbon sources and the build-up of the prokaryote community that occurs as carbon sources are degraded (Figs. 4i-l, 5g-i, 6e and f).

The protist grazer population apparently had a large impact on the number of prokaryotes in the experiments. Protist grazer and prokaryote populations are not independent of each other, as the abundance of one is dependent on the abundance of the other and can show reverse trends when protist grazers are at high levels (Andersen and Fenchel, 1985; Andersen and Sørensen, 1986). Lower threshold levels for protist grazing on prokaryotes (i.e., concentrations below which protist grazing ceases) were reported to range between 5×10^4 and 7×10^5 prokaryotic cells ml^{-1} (Wikner and Hagström, 1991; Sanders et al., 1992; Eccleston-Parry and Leadbeater, 1994; Jeong et al., 2008). In our experiments, prokaryote numbers leveled out at approximately 2×10^5 cells ml^{-1} after heavy grazing (Figs. 4m-p, 5j-l, 6g, h and Table 4). The protist grazers increased in population with a delay of a few days and reached their peak soon after the peak in prokaryote cells. The *Tetraselmis* sp. POC treatment possessed the lowest peak value of prokaryotes seen in any treatment ($\sim 0.5 \times 10^6 \text{ ml}^{-1}$), which was likely partially explained by the fact that it also had the highest number of protist grazers (Fig. 5l and Table 4). The abundance of protist grazers in the 2022 experiment was sufficiently high to rapidly reduce the prokaryote numbers in all experiments to a level of $\sim 2 \times 10^5$ cells ml^{-1} (Figs. 5j-l, 6g and h). The lower feeding threshold is the number of prey items below which prey can no longer be efficiently grazed. For comparison, Andersen and Fenchel (1985) found an experimental numerical response threshold of $1-1.5 \times 10^5$ cells ml^{-1} using samples from Aarhus Bay. Field samples from Azam et al. (1983), Andersen and Sørensen (1986), Wikner and Hagström (1991) and Sanders et al. (1992) showed numerical response thresholds ranging from approximately $2-5 \times 10^5$ cells ml^{-1} .

¹. We are not sure yet as to whether the development of microbial predators – most likely heterotrophic flagellates – affected the carbon degradation itself. Protist grazers are also known to increase the recycling of N and P-rich compounds that may stimulate decay, although more work needs to be done in this regard (Johannes, 1965; Wang et al., 2009). Past studies have concluded that the presence of protist grazers can increase the rate of microbial degradation of organic matter and the extent to which the organic matter is degraded (Ribblett et al., 2005; Risse-Buhl et al., 2015; Chen and Wang, 2018; Chang et al., 2021).

There were also substantial differences in the prokaryote populations between the first and the second *T. weissflogii* POC treatments. There is a much earlier, greater, and more rapid decrease in both ATP and prokaryote abundance in the second treatment. The two biomass indicators show that the first *T. weissflogii* POC treatment had an overall larger microbial population throughout the time period, which may have been responsible for the higher instantaneous decay rates (Figs. 4g, k, o, 5e, h and k). The same algal species was grown under the same conditions, but the mesopelagic water was collected at different times of the year. The water used in the first treatment was taken in October, while the water in the second treatment was taken in May. The observable differences in the development and decline of the microbial communities in the first and second *Thalassiosira weissflogii* POC treatments therefore suggest that they may be a function of the initial microbial communities, such as the number of protist grazers contained within or different predator-prey interactions.

BIOCHEMICAL FRACTIONS

In general, the biochemical compositions in our experiments were similar to other studies that used similar fractionation protocols. A previous study found through shipboard experiments that lipids contained ~18% of the fixed C-14 that was present (Li and Platt, 1982). Even through

experimental manipulation of light levels and water temperature, the percentage of lipids were not greater than 30% of the C-14 total (Li and Platt, 1982). In our experiments, the percentage of lipids in the POC treatments range from ~5% to less than 30% – aside from one outlier (Fig. 8). Prior research has suggested that the biochemical protein fraction is a principal macromolecular component of phytoplankton (~60%) (Wakeham et al., 1997). Proteins have often been assumed to exhibit labile behavior and be subject to fast decay, but proteins have also been identified in the detrital DOM pool that would be harder to digest (Tanoue, 1995; Suzuki et al., 1997; Yamada and Tanoue, 2003; Nunn et al., 2010). The resistance of proteins to decay has been noted in previous literature, but Laursen et al. (1996) describes both labile and harder to degrade proteins (Keil and Kirchman, 1994; DeLong and Béjà, 2010). Protein in our experiments is operationally defined as being TCA-insoluble, while the fractions that are soluble are designated as poly-NA. Therefore, the protein fraction likely consisted of more than just true proteins, and this must be taken into consideration with regard to our data. Similarly, the separation of the lipids via the chloroform-methanol extraction could have included non-lipid substances that could have possibly been degraded more quickly than true lipids.

In the first time interval, lipids and the low molecular weight fraction were more rapidly digested than the structural proteins and polysaccharides (Table 6). These results are in contrast to the degradation experiment in Harvey et al. (1995), where carbohydrates were decayed the fastest, lipids the slowest, and proteins fell in between. There are different lipid classes, the proportion of which in particles has been found to change seasonally (Harvey and Johnston, 1995). It is possible that a labile and easily digestible group of lipids was present initially, such as lipids with short-chain fatty acids (FAs) that generally are easier to degrade than complex lipids (e.g., triglycerides or complex waxes) (Pedrosa-Pàmies et al., 2018). Also, long-chain odd

FAs appear to selectively preserve in the deep sea (Pedrosa-Pàmies et al., 2018). In the experiment with *T. weissflogii* and *Synechococcus* sp, the decay rates associated with the bulk biochemical fractions and each separate fraction were similar between the two species (Harvey et al., 1995). We can confirm this, as the percentages of each biochemical fraction were relatively similar between the three species tested in our experiments. However, Harvey and Macko (1997) found that there were significant differences in the decay of individual lipids between the two types of phytoplankton tested in the previous study. There were even interspecies differences for some of the individual lipids present in both species (Harvey and Macko, 1997). It is possible that in our experiments there were also differences in individual lipid decay among species, but we cannot be sure as we did not separate our lipids into the individual classes. The decay rates were very similar among biochemical fractions in our second time interval, however (Table 6). This finding of relatively static biochemical compositions observed in the later period is more consistent with the non-selective preservation found in other studies (Hedges et al., 2000; Hedges et al., 2001; Lee et al., 2004; Wakeham and Lee, 2019). Conversely, some studies have also shown that aliphatic compounds are selectively preserved with depth (Hwang and Druffel, 2003; Hwang et al., 2006).

FUTURE CARBON CYCLING AND SUMMARY

The carbon cycle is predicted to change with continuing climate change and rising global temperatures, which will impact carbon degradation and the biological pump (Boscolo-Galazzo et al., 2018). The evaluation of recent climate model data predicts changes in POC export at 100 m to be between -1.98 and 0.16 GtC yr^{-1} , depending on the model (Henson et al., 2022). Across 84% of the ocean, the models disagree on whether this change will be positive or negative (Henson et al., 2022). There is more disagreement between the models when comparing the

current POC flux with future predicted fluxes (Henson et al., 2022). DOC trapped in ocean waters can be sequestered on a timescale of years to centuries, keeping it out of the atmosphere and the upper ocean (Hansell et al., 2009). Changes in the marine DOC pools could have drastic impacts on carbon dioxide concentrations in the atmosphere, and as a result, climate change (Kirchman, 2018). It is predicted that the more intense global warming expected in the coming years will reduce the effectiveness of certain processes associated with the biological pump, such as the transport of atmospheric carbon dioxide (Turner, 2015). Increased stratification, decreased nutrient concentrations in the surface layer and as a result decreased amounts of exported carbon are also expected in the oceans with the warming global climate (Turner, 2015). The nature of refractory DOC in intermediate to deep ocean depths, including how it is created as well as its fate, is an area of research that will help shed light on the effects of continued climate change on the oceanic carbon cycle (Baltar et al., 2021). A model created by Boyd (2015) suggests that the factors that will contribute the most to future decreases specifically in POC fluxes are changes in the community structures of algae in the surface layer and zooplankton at depth. We found remarkably consistent decay rates among treatments and experiments. This consistency suggests that neither the composition of the substrate nor the mesopelagic community have major effects on the subsequent decay. Instead, our analysis suggests that a large proportion of the variance in decay rates can be explained by simple compartmentalization into five distinct pools: fresh and refractory pools for each of the POC and DOC fractions as well as the proportion of live material. More research is needed to characterize the biochemical composition of these pools in greater detail and to better understand the regime change from one decay rate to the other.

CONCLUSIONS

In carbon degradation experiments that used mesopelagic water and radiolabeled algal cultures, the treatments with live algal cells initially resisted degradation until a relatively rapid die-off event occurred roughly three weeks into the experiment. In contrast, the POC and DOC fractions were easier for the microbial communities to digest, with the DOC fraction consistently degraded the fastest. All of the treatments displayed clear bi-phasic trends in POC and DOC over time, except for the *E. huxleyi* POC treatment which appeared to maintain a relatively consistent level of first-order decay throughout the entire experiment. The trends in POC differed significantly between each algal species in each phase, however, the differences were not very large, and approximately the same amount of material remained at the end of the experiments. On a more time-resolved level, the carbon decay rates peaked at around three weeks for the live treatments and on the first or second day for all of the dead POC and DOC treatments. These peaks in decay rates were followed closely by peaks in the microbial biomass, seen through both ATP and prokaryote abundances. Protist grazers were also found at high abundances around the times of these microbial peaks, and likely reduced the prokaryote population sizes thereafter. During the first phase of decay, the rate of decay for lipids was greater than the rate of decay for any other biochemical fraction. During the second phase of decay, lipid decay rates were more similar to those of the other fractions and therefore supported the non-selective preservation hypothesis over longer time scales. Based on the results, future avenues of research should focus on the fractionation of sinking material into POC, DOC and live carbon, as well as on the proportion of more easily digestible lipid fractions in the early stages of decay. Particles can sink through a substantial range of depths in the mesopelagic zone during that early period. The separation of sediment trap material into these fractions, rather than attempting to account for

source material, would lead to better predictions of decay rates and would help to better constrain biological pump and vertical carbon flux models.

REFERENCES

- Agusti, S., González-Gordillo, J.I., Vaqué, D., Estrada, M., Cerezo, M.I., Salazar, G., Gasol, J.M., Duarte, C.M., 2015. Ubiquitous healthy diatoms in the deep sea confirm deep carbon injection by the biological pump. *Nat. Commun.* 6, 1–8.
- Alderkamp, A.-C., Buma, A.G.J., van Rijssel, M., 2007. The carbohydrates of *Phaeocystis* and their degradation in the microbial food web. *Biogeochemistry* 83, 99–118.
- Allredge, A., 1998. The carbon, nitrogen and mass content of marine snow as a function of aggregate size. *Deep-Sea Res. I* 45, 529–541.
- Allredge, A.L., 2000. Interstitial dissolved organic carbon (DOC) concentrations within sinking marine aggregates and their potential contribution to carbon flux. *Limnol. Oceanogr.* 45, 1245–1253.
- Andersen, P., Fenchel, T., 1985. Bacterivory by microheterotrophic flagellates in seawater samples. *Limnol. Oceanogr.* 30, 198–202.
- Andersen, P., Sørensen, H.M., 1986. Population dynamics and trophic coupling in pelagic microorganisms in eutrophic coastal waters. *Mar. Ecol. Prog. Ser.* 33, 99–109.
- Azam, F., Fenchel, T., Field, J.G., Gray, J.S., Meyer-Reil, L.A., Thingstad, F., 1983. The Ecological Role of Water-Column Microbes in the Sea. *Mar. Ecol. Prog. Ser.* 10, 257–263.
- Bach, L.T., Strange, P., Taucher, J., Achterberg, E.P., Algueró-Muñiz, M., Horn, H., Esposito, M., Riebesell, U., 2019. The Influence of Plankton Community Structure on Sinking Velocity and Remineralization Rate of Marine Aggregates. *Glob. Biogeochem. Cycles* 33, 971–994.

- Baltar, F., Alvarez-Salgado, X.A., Arístegui, J., Benner, R., Hansell, D.A., Herndl, G.J., Lønborg, C., 2021. What Is Refractory Organic Matter in the Ocean? *Front. Mar. Sci.* 8, 1–7.
- Beaulieu, S.E., 2002. Accumulation and fate of phytodetritus on the sea floor. *Oceanogr. Mar. Biol. Annu. Rev.* 40, 171–232.
- Belcher, A., Iversen, M., Manno, C., Henson, S.A., Tarling, G.A., Sanders, R., 2016a. The role of particle associated microbes in remineralization of fecal pellets in the upper mesopelagic of the Scotia Sea, Antarctica. *Limnol. Oceanogr.* 61, 1049–1064.
- Belcher, A., Iversen, M., Giering, S., Riou, V., Henson, S.A., Berline, L., Guilloux, L., Sanders, R., 2016b. Depth-resolved particle-associated microbial respiration in the northeast Atlantic. *Biogeosciences* 13, 4927–4943.
- Bergauer, K., Fernandez-Guerra, A., Garcia, J.A.L., Sprenger, R.R., Stepanauskas, R., Pachiadaki, M.G., Jensen, O.N., Herndl, G.J., 2017. Organic matter processing by microbial communities throughout the Atlantic water column as revealed by metaproteomics. *Proc. Natl. Acad. Sci. USA* 115, E400–E408.
- Billet, D.S.M., Lampitt, R.S., Rice, A.L., Mantoura, R.F.C., 1983. Seasonal sedimentation of phytoplankton to the deep-sea benthos. *Nature* 302, 520–522.
- Bochdansky, A.B., Bollens, S.M., Rollwagen-Bollens, G.C., Gibson, A.H., 2010. Effect of the heterotrophic dinoflagellate *Oxyrrhis marina* and the copepod *Acartia tonsa* on vertical carbon flux in and around thin layers of the phytoflagellate *Isochrysis galbana*. *Mar. Ecol. Prog. Ser.* 402, 179–196.

- Bochdansky, A.B., 2021. Adenosine triphosphate (ATP) as a metric of microbial biomass in aquatic systems: new simplified protocols, laboratory validation, and a reflection on data from the literature. *Limnol. Oceanogr. Methods* 19, 115–131.
- Boscolo-Galazzo, F., Crichton, K.A., Barker, S., Pearson, P.N., 2018. Temperature dependency of metabolic rates in the upper ocean: A positive feedback to global climate change? *Glob. Planet Change* 170, 201–212.
- Boyd, P.W., 2015. Toward quantifying the response of the oceans' biological pump to climate change. *Front. Mar. Sci.* 2, 1–15.
- Burd, A.B., Hansell, D.A., Steinberg, D.K., Anderson, T.R., Arístegui, J., Baltar, F., Beupré, S.R., Buesseler, K.O., DeHairs, F., Jackson, G.A., Kadko, D.C., Koppelman, R., Lampitt, R.S., Nagata, T., Reinthaler, T., Robinson, C., Robison, B.H., Tamburini, C., Tanaka, T., 2010. Assessing the apparent imbalance between geochemical and biochemical indicators of meso- and bathypelagic biological activity: What the @\$#! is wrong with present calculations of carbon budgets? *Deep-Sea Res. II* 57, 1557–1571.
- Bussmann, I., 1999. Bacterial utilization of humic substances from the Arctic Ocean. *Aquat. Microb. Ecol.* 19, 37–45.
- Cabrera-Brufau, M., Arin, L., Sala, M.M., Cermeño, P., Marrasé, C., 2021. Diatom Dominance Enhances Resistance of Phytoplanktonic POM to Mesopelagic Microbial Decomposition. *Front. Mar. Sci.* 8, 1–17.
- Carlson, C.A., Ducklow, H.W., Hansell, D.A., Smith, Jr., W.O., 1998. Organic carbon partitioning during spring phytoplankton blooms in the Ross Sea polynya and the Sargasso Sea. *Limnol. Oceanogr.* 43, 375–386.

- Carlson, C.A., Hansell, D.A., Nelson, N.B., Siegel, D.A., Smethie, W.M., Khatiwala, S., Meyers, M.M., Halewood, E., 2010. Dissolved organic carbon export and subsequent remineralization in the mesopelagic and bathypelagic realms of the North Atlantic basin. *Deep-Sea Res. II* 57, 1433–1445.
- Caron, D.A., Davis, P.G., Madin, L.P., Sieburth, J.M., 1986. Enrichment of microbial populations in macroaggregates (marine snow) from surface waters of the North Atlantic. *J. Mar. Res.* 44, 543–565.
- Cavan, E.L., Trimmer, M., Shelley, F., Sanders, R., 2017. Remineralization of particulate organic carbon in an ocean oxygen minimum zone. *Nat. Commun.* 8, 1–9.
- Cavan, E.L., Boyd, P.W., 2018. Effect of anthropogenic warming on microbial respiration and particulate organic carbon export rates in the sub-Antarctic Southern Ocean. *Aquat. Microb. Ecol.* 82, 111–127.
- Chang, X., Shi, J., Wang, H., 2021. Spatial modeling and dynamics of organic matter biodegradation in the absence or presence of bacterivorous grazing. *Math. Biosci.* 331, 1–17.
- Chen, S., Wang, D., 2018. Effects of micro-, meio- and macroinvertebrates associated with burial on the decomposition of an aquatic macrophyte (*Vallisneria spiralis*) in a eutrophic shallow lake in China. *Mar. Freshw. Res.* 70, 554–562.
- Collins, J.R., Edwards, B.R., Thamatrakoln, K., Ossolinski, J.E., DiTullio, G.R., Bidle, K.D., Doney, S.C., Van Mooy, A.S., 2015. The multiple fates of sinking particles in the North Atlantic Ocean. *Glob. Biogeochem. Cycles* 29, 1471–1494.
- Conte, M.H., Weber, J.C., 2014. Particle Flux in the Deep Sargasso Sea: The 35–Year Oceanic Flux Program Time Series. *Oceanography* 27, 142–147.

- DeLong, E.F., B ej a, O., 2010. The Light-Driven Proton Pump Proteorhodopsin Enhances Bacterial Survival during Tough Times. *PLoS Biol.* 8, 1–5.
- Ducklow, H.W., Steinberg, D.K., Buesseler, K.O., 2001. Upper Ocean Carbon Export and the Biological Pump. *Oceanography* 14, 50–58.
- Eccleston-Parry, J.D., Leadbeater, B.S.C., 1994. A comparison of the growth kinetics of six marine heterotrophic nanoflagellates fed with one bacterial species. *Mar. Ecol. Prog. Ser.* 105, 167-177.
- Edgington, E.S., Onghena, P., 2020. *Randomization Tests*, 4th ed. Chapman & Hall/CRC, Boca Raton.
- Fallon, R.D., Brock, T.D., 1979. Decomposition of Blue-Green Algal (Cyanobacterial) Blooms in Lake Mendota, Wisconsin. *Appl. Environ. Microbiol.* 37, 820–830.
- Fang, J., Zhang, L., Li, J., Kato, C., Tamburini, C., Zhang, Y.-Z., Dang, H., Guangyi, W., Fengping, W., 2015. The POM-DOM piezophilic microorganism continuum (PDPMC)—The role of piezophilic microorganisms in the global ocean carbon cycle. *Sci. China Earth Sci.* 58, 106–115.
- Finkel, Z.V., Follows, M.J., Irwin, A.J., 2016. Size-scaling of macromolecules and chemical energy content in the eukaryotic microalgae. *J. Plankton Res.* 38, 1151–1162.
- Fontanez, K.M., Eppley, J.M., Samo, T.J., Karl, D.M., DeLong, E.F., 2015. Microbial community structure and function on sinking particles in the North Pacific Subtropical Gyre. *Front. Microbiol.* 6, 1–14.
- Gardner, W.D., 1989. Baltimore Canyon as a modern conduit of sediment to the deep sea. *Deep-Sea Res.* 36, 323–358.

- Garrison, C.E., Bochdansky, A.B., 2015. A simple separation method for downstream biochemical analysis of aquatic microbes. *J. Microbiol. Methods* 111, 78–86.
- Giering, S.L.C., Sanders, R., Lampitt, R.S., Anderson, T.R., Tamburini, C., Boutrif, M., Zubkov, M.V., Marsay, C.M., Henson, S.A., Saw, K., Cook, K., Mayor, D.J., 2014. Reconciliation of the carbon budget in the ocean's twilight zone. *Nature* 507, 480–483.
- Giering, S.L.C., Sanders, R., Martin, A.P., Henson, S.A., Riley, J.S., Marsay, C.M., Johns, D.G., 2017. Particle flux in the oceans: Challenging the steady state assumption. *Glob. Biogeochem. Cycles* 31, 159–171.
- Gillooly, J., Brown, J., West, G., Savage, V., Charnov, E., 2001. Effects of size and temperature on metabolic rate. *Science* 293, 2248–2251.
- Giner, C.R., Pernice, M.C., Balagué, V., Duarte, C.M., Gasol, J.M., Logares, R., Massana, R., 2020. Marked changes in diversity and relative activity of picoeukaryotes with depth in the world ocean. *ISME J.* 14, 437–449.
- Glover, A.G., Gooday, A.J., Bailey, D.M., Billett, D.S.M., Chevaldonne, P., Colaco, A., Copley, J., Cuvelier, D., Desbruyeres, D., Kalogeropoulou, V., Klages, M., Lampadariou, N., Lejeusne, C., Mestre, N.C., Paterson, G.L.J., Perez, T., Ruhl, H., Sarrazin, J., Soltwedel, T., Soto, E.H., Thatje, S., Tselepides, A., Van Gaever, S., Vanreusel, A., 2010. Lesser, M. (Ed.), *Advances in Marine Biology*, vol. 58. Elsevier Academic Press Inc, San Diego, pp. 1–73.
- Golueke, C.G., Oswald, W.J., Gotaas, H.B., 1957. Anaerobic Digestion of Algae. *Appl. Microbiol.* 5, 47–55.
- Gooday, A.J., 2002. Biological Responses to Seasonally Varying Fluxes of Organic Matter to the Ocean Floor: A Review. *J. Oceanogr.* 58, 305–332.

- Guo, R., Liang, Y., Xin, Y., Wang, L., Mou, S., Cao, C., Xie, R., Zhang, C., Tian, J., Zhang, Y., 2018. Insight Into the Pico- and Nano-Phytoplankton Communities in the Deepest Biosphere, the Mariana Trench. *Front. Microbiol.* 9, 1–14.
- Halfter, S., Cavan, E.L., Butterworth, P., Swadling, K.M., Boyd, P.W., 2022. “Sinking dead”—How zooplankton carcasses contribute to particulate organic carbon flux in the subantarctic Southern Ocean. *Limnol. Oceanogr.* 67, 13–25.
- Hansell, D.A., Carlson, C.A., Repeta, D.J., Schlitzer, R., 2009. Dissolved Organic Matter in the Ocean: A Controversy Stimulates New Insights. *Oceanography* 22, 202–211.
- Hansell, D.A., Carlson, C.A., Schlitzer, R., 2012. Net removal of major marine dissolved organic carbon fractions in the subsurface ocean. *Glob. Biogeochem. Cycles* 26, 1–9.
- Hansell, D.A., 2013. Recalcitrant Dissolved Organic Carbon Fractions. *Annu. Rev. Mar. Sci.* 5, 421–445.
- Harvey, H.R., Tuttle, J.H., Bell, J.T., 1995. Kinetics of phytoplankton decay during simulated sedimentation: Changes in biochemical composition and microbial activity under oxic and anoxic conditions. *Geochim. Cosmochim. Acta* 59, 3367–3377.
- Harvey, H.R., Johnston, J.R., 1995. Lipid composition and flux of sinking and size-fractionated particles in Chesapeake Bay. *Org. Geochem.* 23, 751-764.
- Harvey, H.R., Macko, S.A., 1997. Kinetics of phytoplankton decay during simulated sedimentation: changes in lipids under oxic and anoxic conditions. *Org. Geochem.* 27, 129-140.
- Hedges, J.I., Eglinton, G., Hatcher, P.G., Kirchman, D.L., Arnosti, C., Derenne, S., Evershed, R.P., Kögel-Knabner, I., de Leeuw, J.W., Littke, R., Michaelis, W., Rullkötter, J., 2000.

- The molecularly-uncharacterized component of nonliving organic matter in natural environments. *Org. Geochem.* 31, 945–958.
- Hedges, J.I., Baldock, J.A., Gélinas, Y., Lee, C., Peterson, M., Wakeham, S.G., 2001. Evidence for non-selective preservation of organic matter in sinking marine particles. *Nature* 409, 801–804.
- Hegarty, T.W., 1973. Temperature Coefficient (Q_{10}), Seed Germination and Other Biological Processes. *Nature* 243, 305–306.
- Henson, S.A., Laufkötter, C., Leung, S., Giering, S.L.C., Palevsky, H.I., Cavan, E.L., 2022. Uncertain response of ocean biological carbon export in a changing world. *Nat. Geosci.* 15, 248–254.
- Herndl, G.J., Peduzzi, P., 1988. The Ecology of Amorphous Aggregations (Marine Snow) in the Northern Adriatic Sea: I. General Considerations. *Mar. Ecol.* 9, 79–90.
- Herndl, G.J., Bayer, B., Baltar, F., Reinthaler, T., 2023. Prokaryotic Life in the Deep Ocean's Water Column. *Annu. Rev. Mar. Sci.* 15, 5.1–5.23.
- Hobbie, J.E., Daley, R.J., Jasper, S., 1977. Use of Nuclepore Filters for Counting Bacteria by Fluorescence Microscopy. *Appl. Environ. Microbiol.* 33, 1225–1228.
- Holm-Hansen, O., Booth, C.R., 1966. The measurement of adenosine triphosphate in the ocean and its ecological significance: Adenosine triphosphate in the ocean. *Limnol. Oceanogr.* 11, 510–519.
- Holm-Hansen, O., 1969. Determination of Microbial Biomass in Ocean Profiles. *Limnol. Oceanogr.* 14, 740-747.
- Hwang, J., Druffel, E.R.M., 2003. Lipid-Like Material as the Source of the Uncharacterized Organic Carbon in the Ocean? *Science* 299, 881–884.

- Hwang, J., Druffel, E.R.M., Eglinton, T.I., Repeta, D.J., 2006. Source(s) and cycling of the nonhydrolyzable organic fraction of oceanic particles. *Geochim. Cosmochim. Acta* 70, 5162–5168.
- Ivars-Martinez, E., Martin-Cuadrado, A.-B., D’Auria, G., Mira, A., Ferriera, S., Johnson, J., Friedman, R., Rodriguez-Valera, F., 2008. Comparative genomics of two ecotypes of the marine planktonic copiotroph *Alteromonas macleodii* suggests alternative lifestyles associated with different kinds of particulate organic matter. *ISME J.* 2, 1194–1212.
- Iversen, M.H., Ploug, H., 2010. Ballast minerals and the sinking carbon flux in the ocean: carbon-specific respiration rates and sinking velocity of marine snow aggregates. *Biogeosciences* 7, 2613–2624.
- Iversen, M.H., Ploug, H., 2013. Temperature effects on carbon-specific respiration rate and sinking velocity of diatom aggregates - potential implications for deep ocean export processes. *Biogeosciences* 10, 4073–4085.
- Iversen, M.H., Lampitt, R.S., 2020. Size does not matter after all: No evidence for a size-sinking relationship for marine snow. *Prog. Oceanogr.* 189, 1–7.
- Jeong, H.J., Seong, K.A., Yoo, Y.D., Kim, T.H., Kang, N.S., Kim, S., Park, J.Y., Kim, J.S., Kim, G.H., Song, J.Y., 2008. Feeding and Grazing Impact by Small Marine Heterotrophic Dinoflagellates on Heterotrophic Bacteria. *J. Eukaryot. Microbiol.* 55, 271-288.
- Jiao, N., Herndl, G.J., Hansell, D.A., Benner, R., Kattner, G., Wilhelm, S.W., Kirchman, D.L., Weinbauer, M.G., Luo, T., Chen, F., Azam, F., 2010. Microbial production of recalcitrant dissolved organic matter: long-term carbon storage in the global ocean. *Nat. Rev. Microbiol.* 8, 593–599.

- Johannes, R.E., 1965. Influence of marine protozoa on nutrient regeneration. *Limnol. Oceanogr.* 10, 434–442.
- Karl, D.M., Church, M.J., Dore, J.E., Letelier, R.M., Mahaffey, C., 2012. Predictable and efficient carbon sequestration in the North Pacific Ocean supported by symbiotic nitrogen fixation. *Proc. Natl. Acad. Sci. USA* 109, 1842–1849.
- Keil, R.G., Kirchman, D.L., 1994. Abiotic transformation of labile protein to refractory protein in sea water. *Mar. Chem.* 45, 187–196.
- Kheireddine, M., Dall’Olmo, G., Ouhssain, M., Krokos, G., Claustre, H., Schmechtig, C., Poteau, A., Zhan, P., Hoteit, I., Jones, B.H., 2020. Organic Carbon Export and Loss Rates in the Red Sea. *Glob. Biogeochem. Cycles* 34, 1–20.
- Kieft, B., Li, Z., Bryson, S., Hettich, R.L., Pan, C., Mayali, X., Mueller, R.S., 2021. Phytoplankton exudates and lysates support distinct microbial consortia with specialized metabolic and ecophysiological traits. *Proc. Natl. Acad. Sci. USA* 118, 1–12.
- Kirchman, D.L., 2018. Degradation of organic matter. In: *Processes in Microbial Ecology*, 2nd ed. Oxford Univ. Press, Oxford, pp. 113–132.
- Lampitt, R.S., 1985. Evidence for the seasonal deposition of detritus to the deep-sea floor and its subsequent resuspension. *Deep-Sea Res.* 32, 885–897.
- Laursen, A.K., Mayer, L.M., Townsend, D.W., 1996. Lability of proteinaceous material in estuarine seston and subcellular fractions of phytoplankton. *Mar. Ecol. Prog. Ser.* 136, 227–234.
- Lee, C., Murray, D.W., Barber, R.T., Buesseler, K.O., Dymond, J., Hedges, J.I., Honjo, S., Manganini, S.J., Marra, J., Moser, C., Peterson, M.L., Prell, W.L., Wakeham, S.G., 1998.

- Particulate organic carbon fluxes: compilation of results from the 1995 US JGOFS Arabian Sea Process Study. *Deep-Sea Res. II* 45, 2489–2501.
- Lee, C., Wakeham, S., Arnosti, C., 2004. Particulate Organic Matter in the Sea: The Composition Conundrum. *Ambio* 33, 565–575.
- Lee, S., Fuhrman, J.A., 1987. Relationships between Biovolume and Biomass of Naturally Derived Marine Bacterioplankton. *Appl. Environ. Microbiol.* 53, 1298-1303.
- Lefèvre, D., Denis, M., Lambert, C.E., Miquel, J.-C., 1996. Is DOC the main source of organic matter remineralization in the ocean water column? *J. Mar. Syst.* 7, 281–291.
- Liu, H., Guo, Y., Yun, M., Wu, C., Xu, W., Zhang, X., Thangaraj, S., Sun, J., 2022. Massive presence of intact microalgal cells in the deep ocean near 5°N of the eastern Indian Ocean. *Mar. Biol.* 169, 1–13.
- Li, W.K.W., Glover, H.E., Morris, I., 1980. Physiology of carbon photoassimilation by *Oscillatoria thiebautii* in the Caribbean Sea. *Limnol. Oceanogr.* 25, 447–456.
- Li, W.K.W., Platt, T., 1982. Distribution of carbon among photosynthetic end-products in phytoplankton of the eastern Canadian Arctic. *J. Phycol.* 18, 466–471.
- Lønborg, C., Álvarez-Salgado, X.A., Letscher, R.T., Hansell, D.A., 2018. Large Stimulation of Recalcitrant Dissolved Organic Carbon Degradation by Increasing Ocean Temperatures. *Front. Mar. Sci.* 4, 1–11.
- Lopez, C.N., Robert, M., Galbraith, M., Bercovici, S.K., Orellana, M.V., Hansell, D.A., 2020. High Temporal Variability of Total Organic Carbon in the Deep Northeastern Pacific. *Front. Earth Sci.* 8, 1–11.

- McDonnell, A.M.P., Boyd, P.W., Buesseler, K.O., 2015. Effects of sinking velocities and microbial respiration rates on the attenuation of particulate carbon fluxes through the mesopelagic zone. *Glob. Biogeochem. Cycles* 29, 175–193.
- Menden-Deuer, S., Lessard, E.J., 2000. Carbon to volume relationships for dinoflagellates, diatoms, and other protist plankton. *Limnol. Oceanogr.* 45, 569-579.
- Meon, B., Kirchman, D.L., 2001. Dynamics and molecular composition of dissolved organic material during experimental phytoplankton blooms. *Mar. Chem.* 75, 185–199.
- Møller, E.F., Thor, P., Nielsen, T.G., 2003. Production of DOC by *Calanus finmarchicus*, *C. glacialis* and *C. hyperboreus* through sloppy feeding and leakage from fecal pellets. *Mar. Ecol. Prog. Ser.* 262, 185–191.
- Morata, N., Seuthe, L., 2014. Importance of bacteria and protozooplankton for faecal pellet degradation. *Oceanologia* 56, 565–581.
- Nagata, T., 2008. Organic Matter–Bacteria Interactions in Seawater. In: Kirchman, D.L. (Ed.), *Microbial Ecology of the Oceans*, 2nd ed. John Wiley & Sons, Inc., Hoboken, pp. 207–241.
- Nielsen, E.S., 1955. The production of antibiotics by plankton algae and its effect upon bacterial activities in the sea. *Deep-Sea Res.* 3 [Suppl.], 281–286.
- Nodder, S.D., Duineveld, G.C.A., Pilditch, C.A., Sutton, P.J., Probert, P.K., Lavaleye, M.S.S., Witbaard, R., Chang, F.H., Hall, J.A., Richardson, K.M., 2007. Focusing of phytodetritus deposition beneath a deep-ocean front, Chatham Rise, New Zealand. *Limnol. Oceanogr.* 52, 299–314.

- Nunn, B.L., Ting, Y.S., Malmström, L., Tsai, Y.S., Squier, A., Goodlett, D.R., Harvey, H.R., 2010. The path to preservation: Using proteomics to decipher the fate of diatom proteins during microbial degradation. *Limnol. Oceanogr.* 55, 1790–1804.
- Ogawa, H., Amagai, Y., Koike, I., Kaiser, K., Benner, R., 2001. Production of Refractory Dissolved Organic Matter by Bacteria. *Science* 292, 917–920.
- Ogura, N., 1975. Further Studies on Decomposition of Dissolved Organic Matter in Coastal Seawater. *Mar. Biol.* 31, 101–111.
- Omand, M.M., Govindarajan, R., He, J., Mahadevan, A., 2020. Sinking flux of particulate organic matter in the oceans: Sensitivity to particle characteristics. *Sci. Rep.* 10, 1–16.
- Oppenheimer, C.H., Vance, M.H., 1960. Attachments of Bacteria to the Surfaces of Living and Dead Microorganisms in Marine Sediments (Attachment of Bacteria to Microorganisms). *Z. Allg. Mikrobiol.* 1, 47–52.
- Pedler, B.E., Aluwihare, L.I., Azam, F., 2014. Single bacterial strain capable of significant contribution to carbon cycling in the surface ocean. *Proc. Natl. Acad. Sci. USA* 111, 7202–7207.
- Pedrosa-Pàmies, R., Conte, M.H., Weber, J.C., Johnson, R., 2018. Carbon cycling in the Sargasso Sea water column: Insights from lipid biomarkers in suspended particles. *Prog. Oceanogr.* 168, 248–278.
- Ploug, H., Grossart, H.P., 2000. Bacterial growth and grazing on diatom aggregates: Respiratory carbon turnover as a function of aggregate size and sinking velocity. *Limnol. Oceanogr.* 45, 1467–1475.

- Ploug, H., Iversen, M.H., Koski, M., Buitenhuis, E.T., 2008. Production, oxygen respiration rates, and sinking velocity of copepod fecal pellets: Direct measurements of ballasting by opal and calcite. *Limnol. Oceanogr.* 53, 469–476.
- Ploug, H., Bergkvist, J., 2015. Oxygen diffusion limitation and ammonium production within sinking diatom aggregates under hypoxic and anoxic conditions. *Mar. Chem.* 176, 142–149.
- Porter, K.G., Feig, Y.S., 1980. The Use of DAPI for Identifying and Counting Aquatic Microflora. *Limnol. Oceanogr.* 25, 943–948.
- Reinthaler, T., van Aken, H.M., Herndl, G.J., 2010. Major contribution of autotrophy to microbial carbon cycling in the deep North Atlantic's interior. *Deep-Sea Res. II* 57, 1572–1580.
- Ribblett, S.G., Palmer, M.A., Coats, D.W., 2005. The importance of bacterivorous protists in the decomposition of stream leaf litter. *Freshw. Biol.* 50, 516–526.
- Risse-Buhl, U., Schlief, J., Mutz, M., 2015. Phagotrophic protists are a key component of microbial communities processing leaf litter under contrasting oxic conditions. *Freshw. Biol.* 60, 2310–2322.
- Rivkin, R.B., 1985. Carbon-14 labelling patterns of individual marine phytoplankton from natural populations. *Mar. Biol.* 89, 135–142.
- Sanders, R.W., Caron, D.A., Berninger, U.-G., 1992. Relationships between bacteria and heterotrophic nanoplankton in marine and fresh waters: an inter-ecosystem comparison. *Mar. Ecol. Prog. Ser.* 86, 1–14.
- Seiki, T., Date, E., Izawa, H., 1991. Decomposition Characteristics of Particulate Organic Matter in Hiroshima Bay. *J. Oceanogr. Soc. Japan* 47, 207–220.

- Siegel, D.A., Buesseler, K.O., Behrenfeld, M.J., Benitez-Nelson, C.R., Boss, E., Brzezinski, M.A., Burd, A., Carlson, C.A., D'Asaro, E.A., Doney, S.C., Perry, M.J., Stanley, R.H.R., Steinberg, D.K., 2016. Prediction of the Export and Fate of Global Ocean Net Primary Production: The EXPORTS Science Plan. *Front. Mar. Sci.* 3, 1–10.
- Siegel, D.A., DeVries, T., Cetinić, I., Bisson, K.M., 2023. Quantifying the Ocean's Biological Pump and Its Carbon Cycle Impacts on Global Scales. *Annu. Rev. Mar. Sci.* 15, 329-356.
- Silver, M.W., Shanks, A.L., Trent, J.D., 1978. Marine Snow: Microplankton Habitat and Source of Small-Scale Patchiness in Pelagic Populations. *Science* 201, 371–373.
- Silver, M.W., Coale, S.L., Pilskaln, C.H., Steinberg, D.R., 1998. Giant aggregates: Importance as microbial centers and agents of material flux in the mesopelagic zone. *Limnol. Oceanogr.* 43, 498–507.
- Simon, M., Grossart, H.-P., Schweitzer, B., Ploug, H., 2002. Microbial ecology of organic aggregates in aquatic ecosystems. *Aquat. Microb. Ecol.* 28, 175–211.
- Smith Jr., K.L., Ruhl, H.A., Huffard, C.L., Messié, M., Kahru, M., 2018. Episodic organic carbon fluxes from surface ocean to abyssal depths during long-term monitoring in NE Pacific. *Proc. Natl. Acad. Sci. USA* 115, 12235–12240.
- Suroy, M., Panagiotopoulos, C., Boutorh, J., Goutx, M., Moriceau, B., 2015. Degradation of diatom carbohydrates: A case study with N- and Si-stressed *Thalassiosira weissflogii*. *J. Exp. Mar. Biol. Ecol.* 470, 1–11.
- Suzuki, S., Kogure, K., Tanoue, E., 1997. Immunochemical detection of dissolved proteins and their source bacteria in marine environments. *Mar. Ecol. Prog. Ser.* 158, 1–9.
- Szewczyk, C.J., Smith, E.M., Benitez-Nelson, C.R., 2023. Temperature sensitivity of oxygen demand varies as a function of organic matter source. *Front. Mar. Sci.* 10, 1–12.

- Tanoue, E., 1995. Detection of dissolved protein molecules in oceanic waters. *Mar. Chem.* 51, 239–252.
- Taylor, G.T., 1989. Variability in the vertical flux of microorganisms and biogenic material in the epipelagic zone of a North Pacific central gyre station. *Deep-Sea Res.* 36, 1287–1308.
- Taylor, G.T., Way, J., Scranton, M.I., 2003. Planktonic carbon cycling and transport in surface waters of the highly urbanized Hudson River estuary. *Limnol. Oceanogr.* 48, 1779–1795.
- Tian, R.C., Vézina, A.F., Deibel, D., Rivkin, R.B., 2003. Sensitivity of biogenic carbon export to ocean climate in the Labrador Sea, a deep-water formation region. *Glob. Biogeochem. Cycles* 17, 1–11.
- Tréguer, P., Legendre, L., Rivkin, R.T., Ragueneau, O., Dittert, N., 2003. Water Column Biogeochemistry below the Euphotic Zone. In: Fasham, J.R.M. (Ed.), *Ocean Biogeochemistry: A Synthesis of the Joint Global Ocean Flux Study (JGOFS)*. Springer-Verlag, Berlin, pp. 145–156.
- Tréguer, P., Bowler, C., Moriceau, B., Dutkiewicz, S., Gehlen, M., Aumont, O., Bittner, L., Dugdale, R., Finkel, Z., Iudicone, D., Jahn, O., Guidi, L., Lasbleiz, M., Leblanc, K., Levy, M., Pondaven, P., 2018. Influence of diatom diversity on the ocean biological carbon pump. *Nat. Geosci.* 11, 27–37.
- Turner, J.T., 2015. Zooplankton fecal pellets, marine snow, phytodetritus and the ocean's biological pump. *Prog. Oceanogr.* 130, 205–248.
- Vallance, C., 2017. *An Introduction to Chemical Kinetics*. Morgan & Claypool Publishers, San Rafael.

- van 't Hoff, J.H., 1899. Influence of Temperature on Velocity of Reaction. In: Lehfeldt, R.A. (Trans.), Lectures on Theoretical and Physical Chemistry: Part I. Chemical Dynamics. Edward Arnold, London, pp. 225–236.
- Vardi, A., Haramaty, L., Van Mooy, B.A.S., Fredricks, H.F., Kimmance, S.A., Larsen, A., Bidle, K.D., 2012. Host–virus dynamics and subcellular controls of cell fate in a natural coccolithophore population. *Proc. Natl. Acad. Sci. USA* 109, 19327–19332.
- Vlahos, P., Chen, R.F., Repeta, D.J., 2002. Dissolved organic carbon in the Mid-Atlantic Bight. *Deep-Sea Res. Part II Top. Stud. Oceanogr.* 49, 4369–4385.
- Wakeham, S.G., Lee, C., 1993. Production, Transport, and Alteration of Particulate Organic Matter in the Marine Water Column. In: Engel, M.H., Macko, S.A. (Eds.), *Organic Geochemistry*. Plenum Press, New York, pp. 145–169.
- Wakeham, S.G., Lee, C., Hedges, J.I., Hernes, P.J., Peterson, M.J., 1997. Molecular indicators of diagenetic status in marine organic matter. *Geochim. Cosmochim. Acta* 61, 5363–5369.
- Wakeham, S.G., Lee, C., 2019. Limits of our knowledge, part 2: Selected frontiers in marine organic biogeochemistry. *Mar. Chem.* 212, 16–46.
- Waksman, S.A., Stokes, J.L., Butler, M.R., 1937. Relation of Bacteria to Diatoms In Sea Water. *J. Mar. Biol. Assoc.* 22, 359–373.
- Walsh, I., Dymond, J., Collier, R., 1988. Rates of recycling of biogenic components of settling particles in the ocean derived from sediment trap experiments. *Deep-Sea Res.* 35, 43–58.
- Wang, H., Jiang, L., Weitz, J.S., 2009. Bacterivorous grazers facilitate organic matter decomposition: a stoichiometric modeling approach. *FEMS Microbiol. Ecol.* 69, 170–179.

- Westrich, J.T., Berner, R.A., 1984. The role of sedimentary organic matter in bacterial sulfate reduction: The G model tested. *Limnol. Oceanogr.* 29, 236–249.
- Wikner, J., Hagström, Å., 1991. Annual study of bacterioplankton community dynamics. *Limnol. Oceanogr.* 36, 1313–1324.
- Yamada, N., Tanoue, E., 2003. Detection and partial characterization of dissolved glycoproteins in oceanic waters. *Limnol. Oceanogr.* 48, 1037–1048.
- Zhao, H., Zhang, Z., Nair, S., Zhao, J., Mou, S., Xu, K., Zhang, Y., 2022. Vertically Exported Phytoplankton (< 20 μm) and Their Correlation Network With Bacterioplankton Along a Deep-Sea Seamount. *Front. Mar. Sci.* 9, 1–15.
- Zweifel, U.L., Hagström, Å., 1995. Total Counts of Marine Bacteria Include a Large Fraction of Non-Nucleoid-Containing Bacteria (Ghosts). *Appl. Environ. Microbiol.* 61, 2180–2185.

APPENDIX

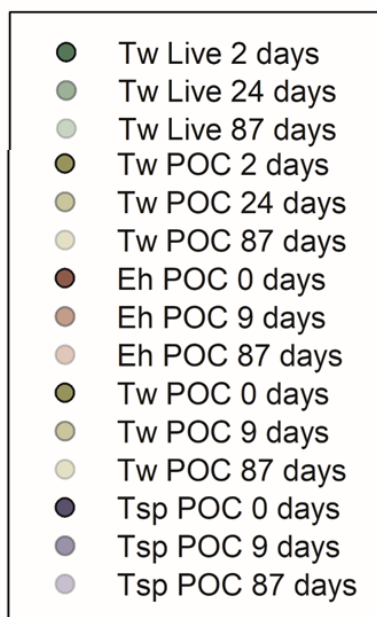
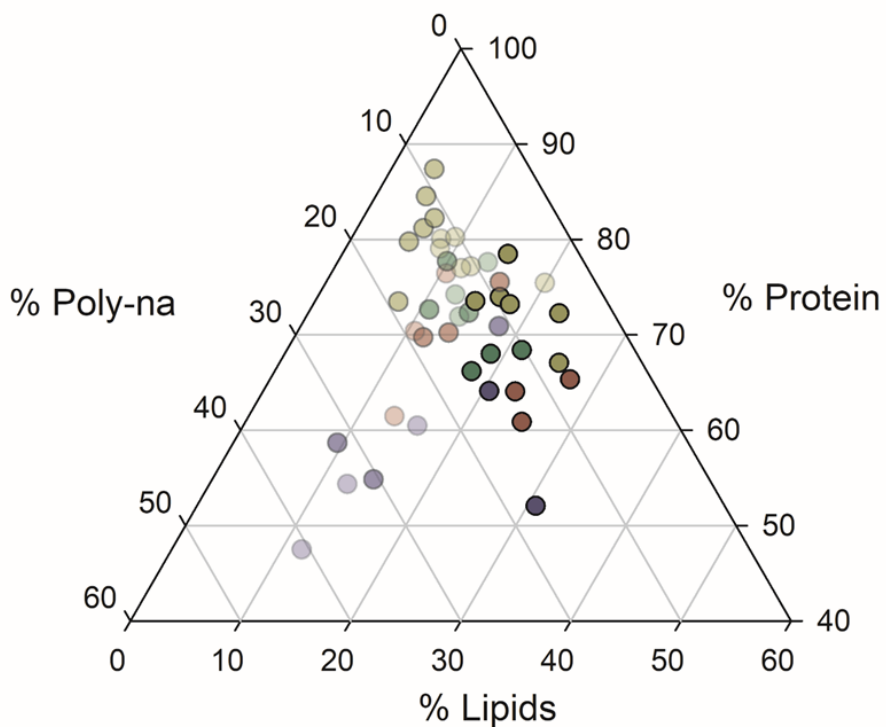


Fig. S1. Biochemical fractionations of samples taken from POC treatments, at three time points during the experimental time frames. Green represents sample values from the 12 °C live *T. weissflogii* (Tw Live) treatment, olive the *T. weissflogii* POC (Tw POC) treatment, red-brown the *E. huxleyi* POC (Eh POC) treatment and violet the *Tetraselmis* sp. POC (Tsp POC) treatment. The degree of shading indicates the degree of decay, with opaque shades being undecayed and more transparent shades being more strongly decayed. The number of days refers to the number of days elapsed since the addition of each treatment to the mesopelagic water.

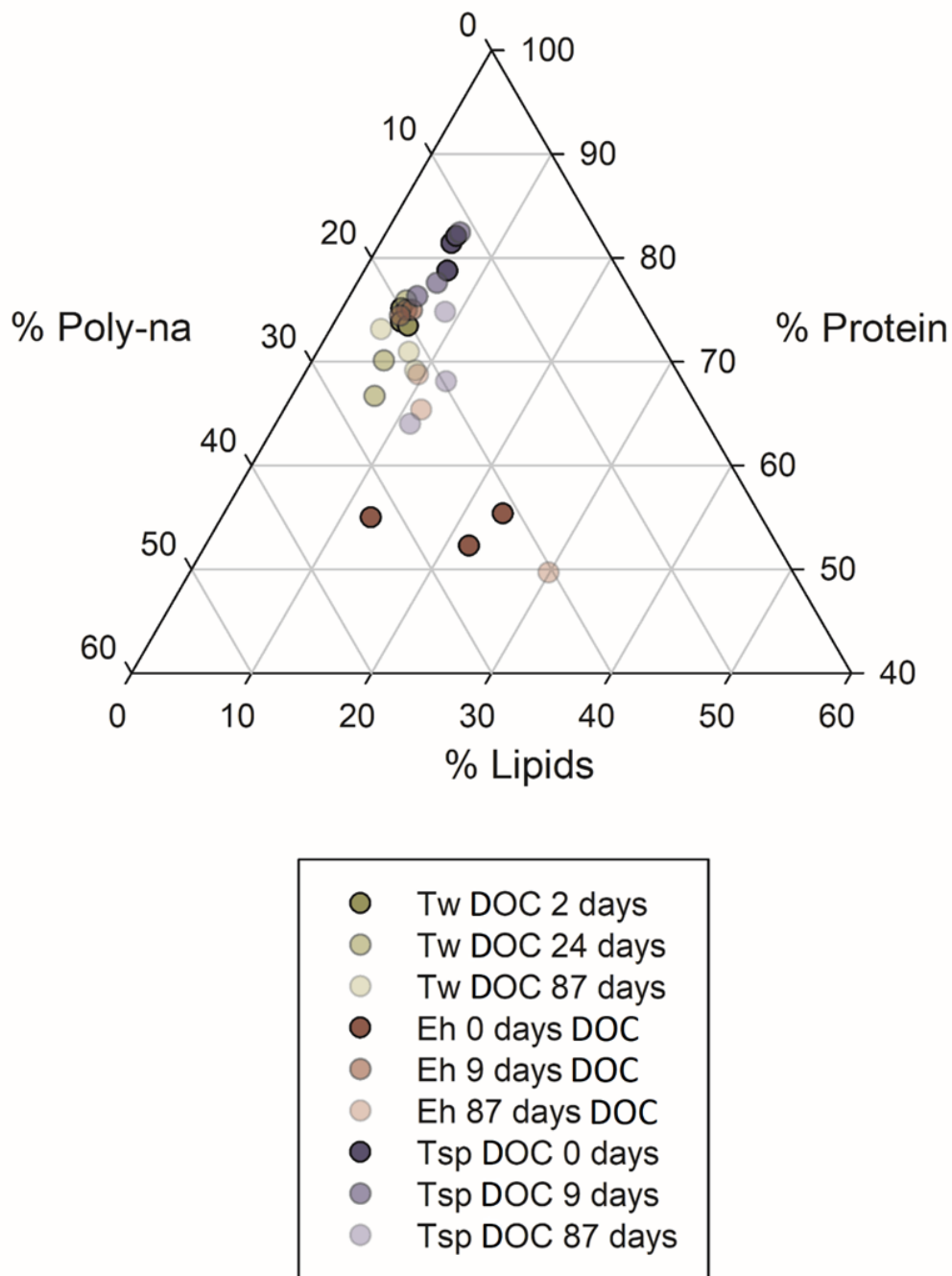


Fig. S2. Biochemical fractionations of samples taken from DOC treatments, at three time points during the experimental time frames. Olive represents sample values from the *T. weissflogii* DOC (Tw DOC) treatment, red-brown the *E. huxleyi* DOC (Eh DOC) treatment and violet the *Tetraselmis* sp. DOC (Tsp DOC) treatment. The degree of shading indicates the degree of decay, with opaque shades being undecayed and more transparent shades being more strongly decayed. The number of days refers to the number of days elapsed since the addition of each treatment to the mesopelagic water. Note that this fractionation represents the POC fraction in the DOC experiments and thus the microbial community, rather than the original growth substrate.

VITA

Noah Jonathan Craft
Department of Ocean & Earth Sciences
Old Dominion University
Norfolk, VA 23529

EDUCATION

B.S. (May 2020) in Earth and Environmental Sciences, Virginia Wesleyan University, 5817 Wesleyan Dr, Virginia Beach, VA 23455

M.S. (Expected December 2023) in Ocean and Earth Sciences, Old Dominion University, 5115 Hampton Blvd, Norfolk, VA 23529

PROFESSIONAL EXPERIENCE

2021-2022, Graduate Research Assistant, Old Dominion University, Norfolk VA 23529

2020-2023, Graduate Teaching Assistant, Old Dominion University, Norfolk VA 23529

CONFERENCE PRESENTATIONS

N. Craft, "Using ^{14}C -labeled Diatoms to Measure the Degradation of Carbon in the Mesopelagic Zone" Oral presentation delivered at the Ocean Sciences Meeting, Virtual. March 2022

N. Craft, "Carbon Degradation by a Mesopelagic Microbial Community: Following Particulate Organic Carbon and Biomass Over Time With Three Types of Carbon-14-Labeled Algae" Poster presentation delivered at the Association for the Sciences of Limnology and Oceanography Aquatic Sciences Meeting, Spain. June 2023